NATIONAL CENTRAL UNIVERSITY

GRADUATE INSTITUTE OF APPLIED GEOLOGY

Progress Report

Monitoring land subsidence in the Choushui River Fluvial Plain by utilizing the SBAS-PSInSAR method

2023/4/7

Advisor: Prof. Chuen-Fa, Ni

Student: David (阮蔡榮長)

What is land subsidence?

- Land surface sinking/settlement
- Vertical downward movement
- Not include *landslides*

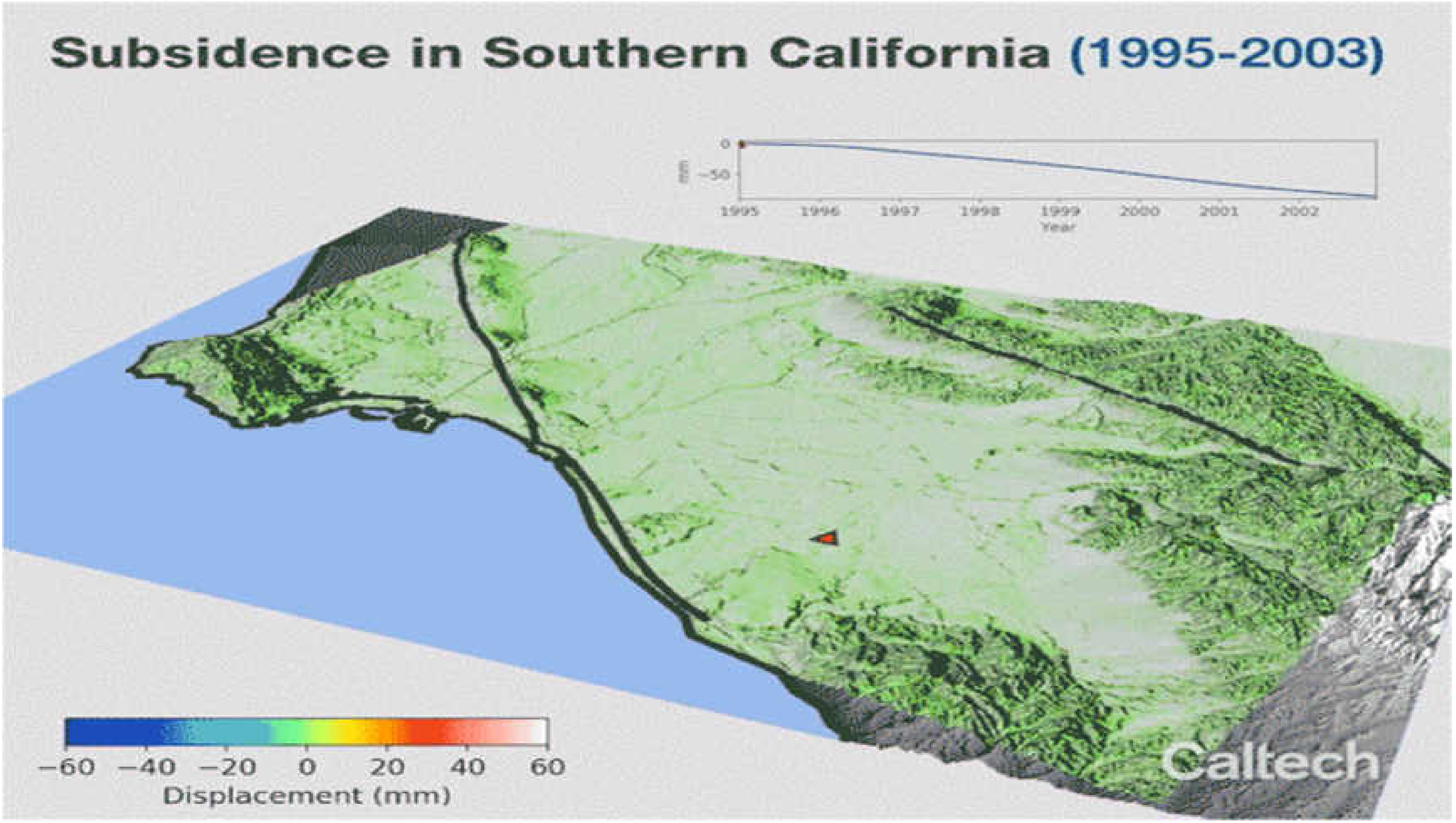

Study Area

- Choushui River Fluvial Plain (in central region of Taiwan)
- Important agricultural area
- Groundwater for irrigation → Overextraction
- Land subsidence → Affect human lives and infrastructures

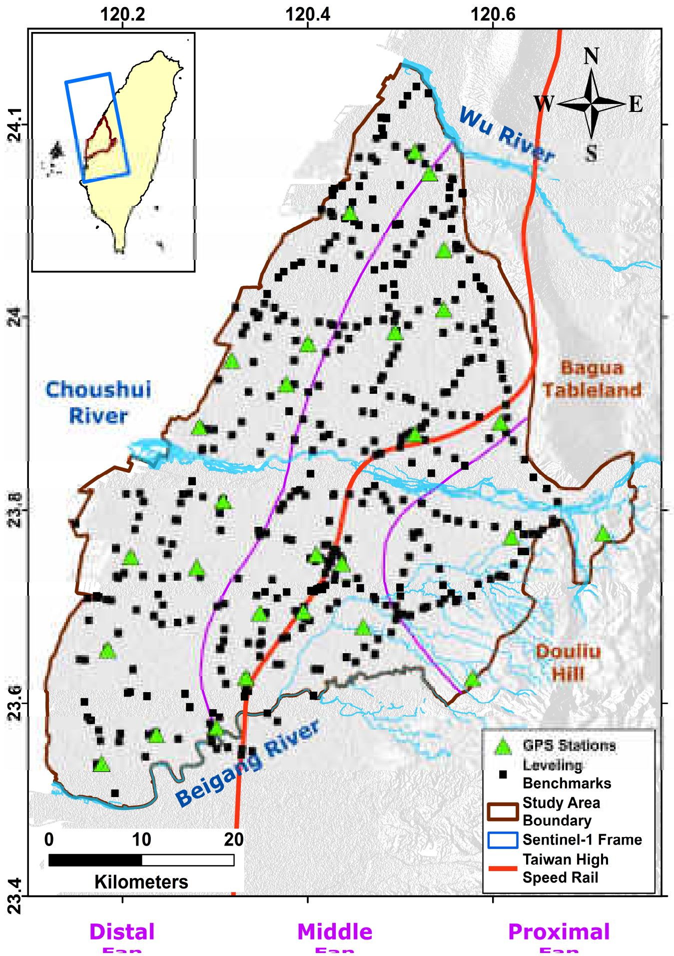

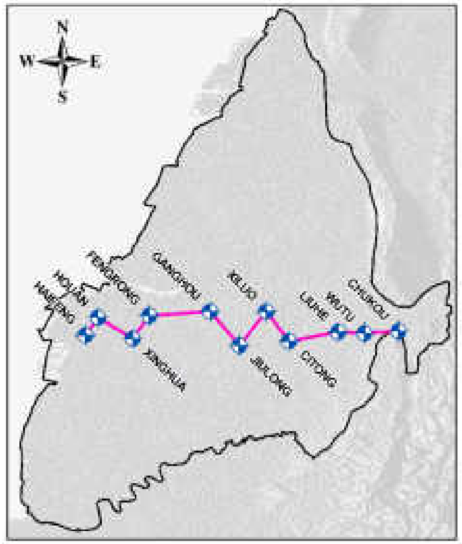

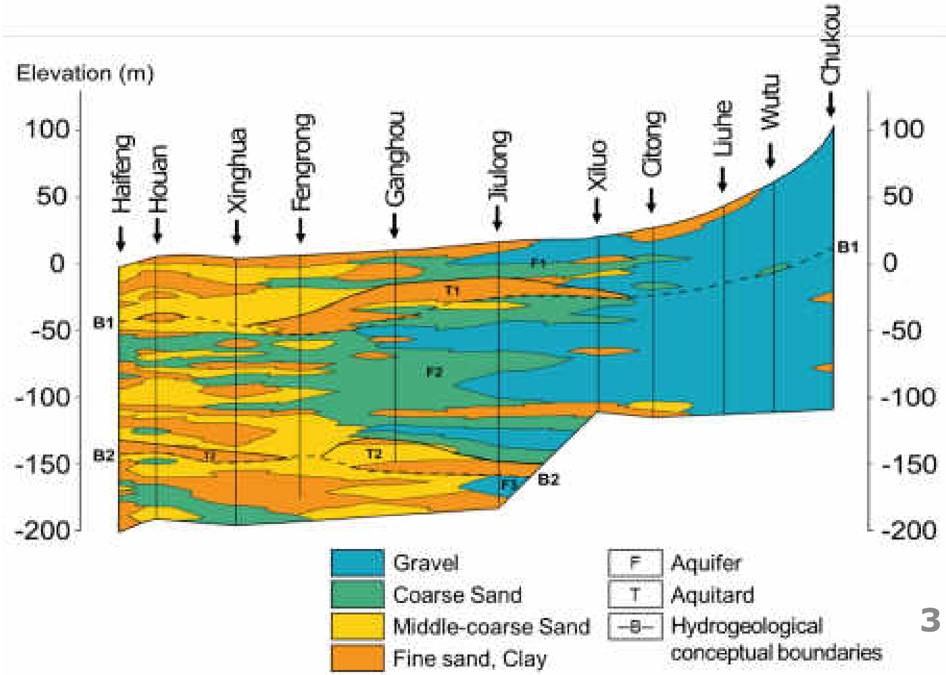

Current Monitoring Networks

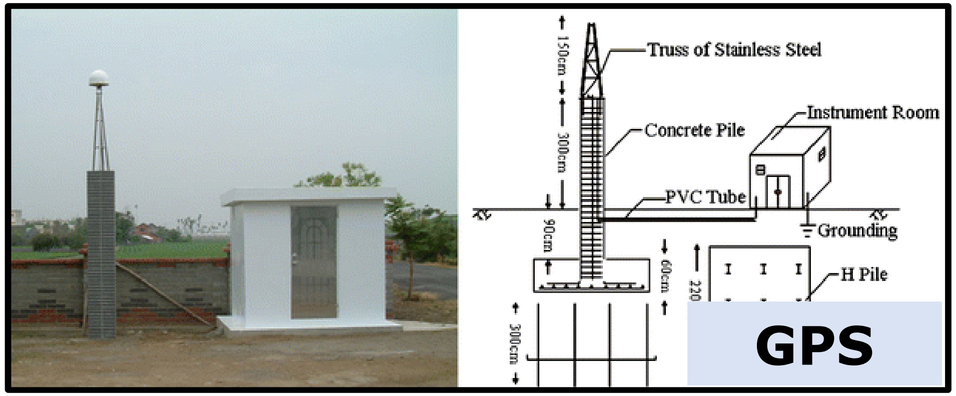

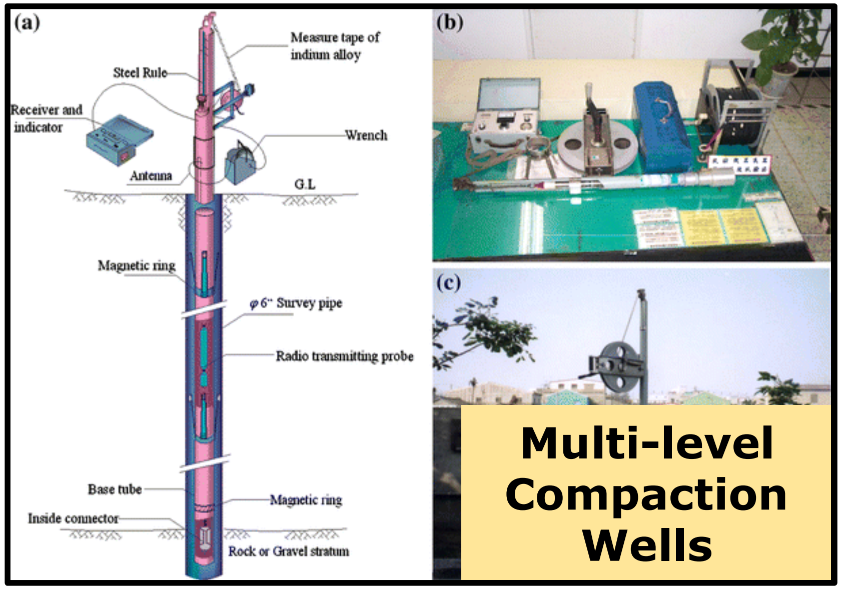

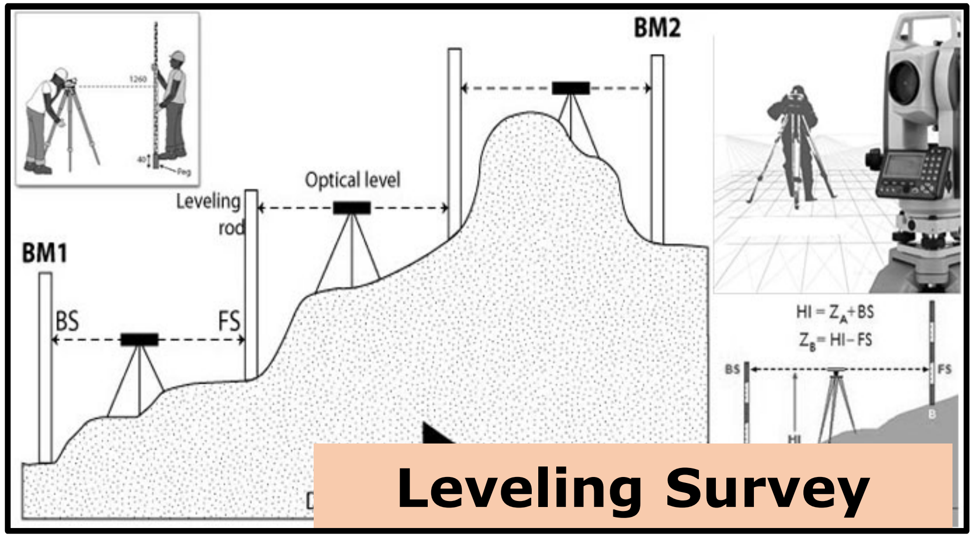

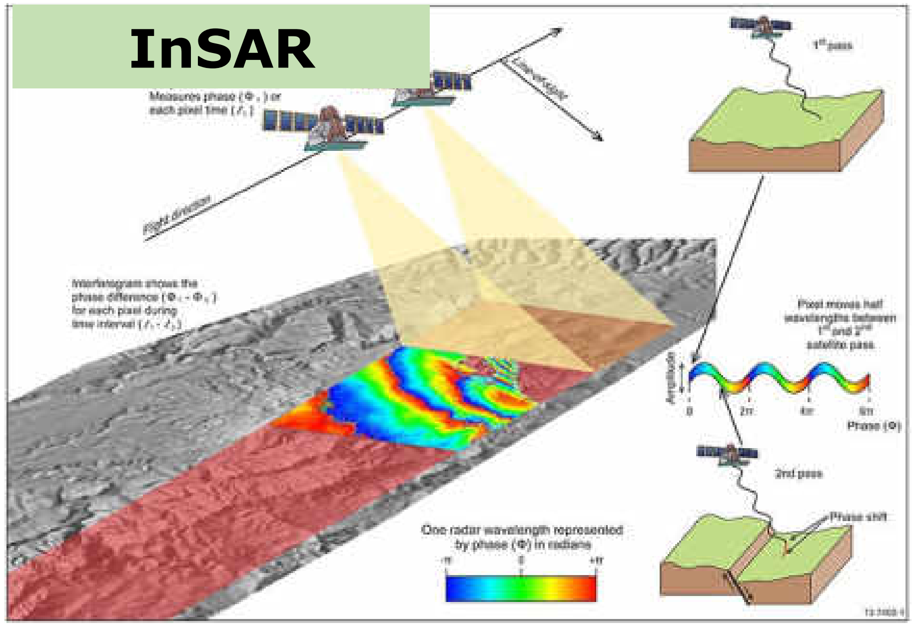

Research Motivations

Traditional Monitoring Method Drawbacks

- GPS → Costly installation
- Leveling → Time-consuming
- Point-wise measurements
- Imply errors when interpolating values between points

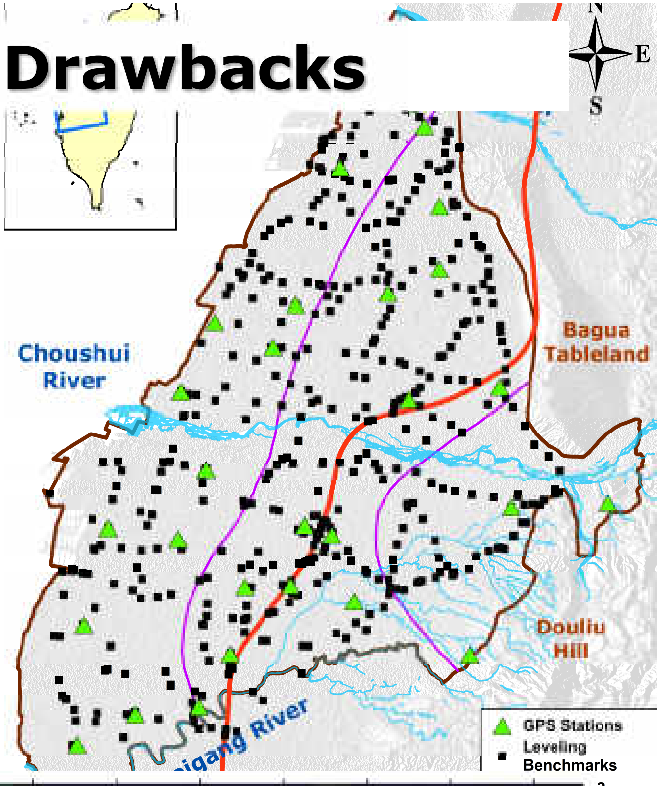

SAR images and InSAR-based techniques

- Large coverage
- High visiting frequency
- Free data (Sentinel-1)

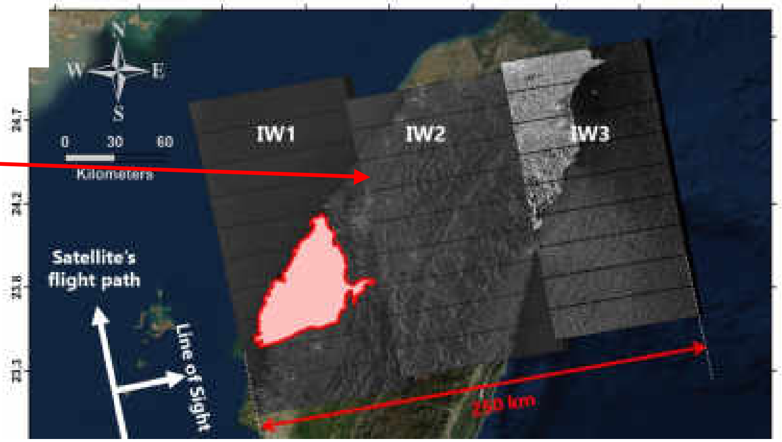

Research Motivations

Previous study inadequacies

- SBAS-InSAR only → phase unwrapping errors & time consuming
- Ignoring horizontal motions → simplify workflow

$$\delta_{vert} = \frac{\delta_{LOS}}{\cos\theta}$$

$$(\theta: incidence\ angle)$$

- Not showing deformation time series or subsidence profiles

Objectives

- Recent surface deformation in CRFP, 2016 – 2022
- Consider horizontal movements during calibration process
- Deformation time series in subsiding areas
- Show the subsidence profile along and across THSR

Optical satellite images & SAR images difference?

Different energy sources

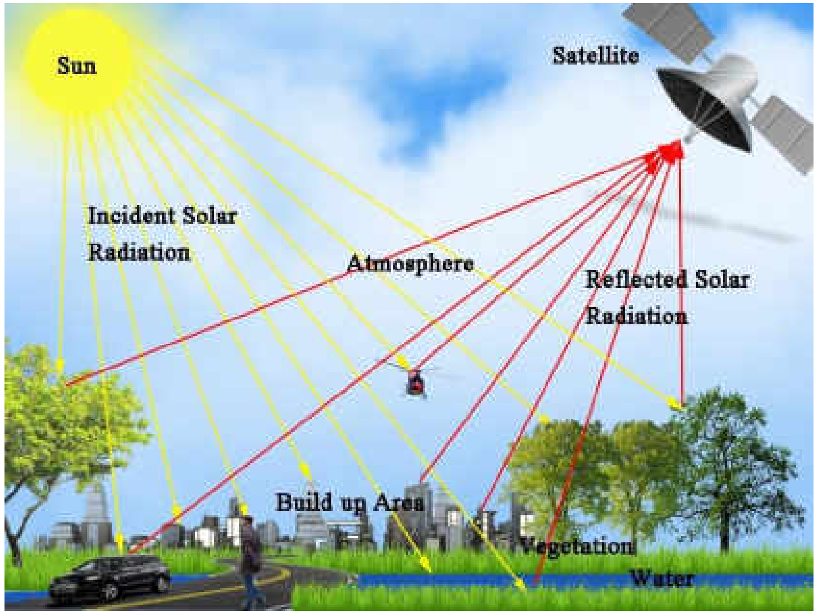

Optical images

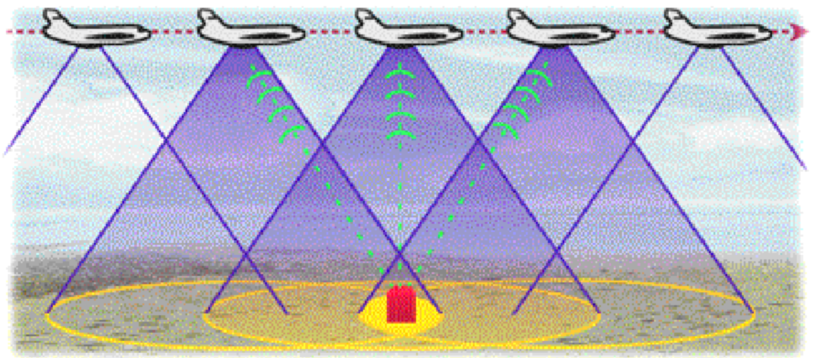

SAR* images

SAR : Synthetic Aperture Radar

Phase Difference

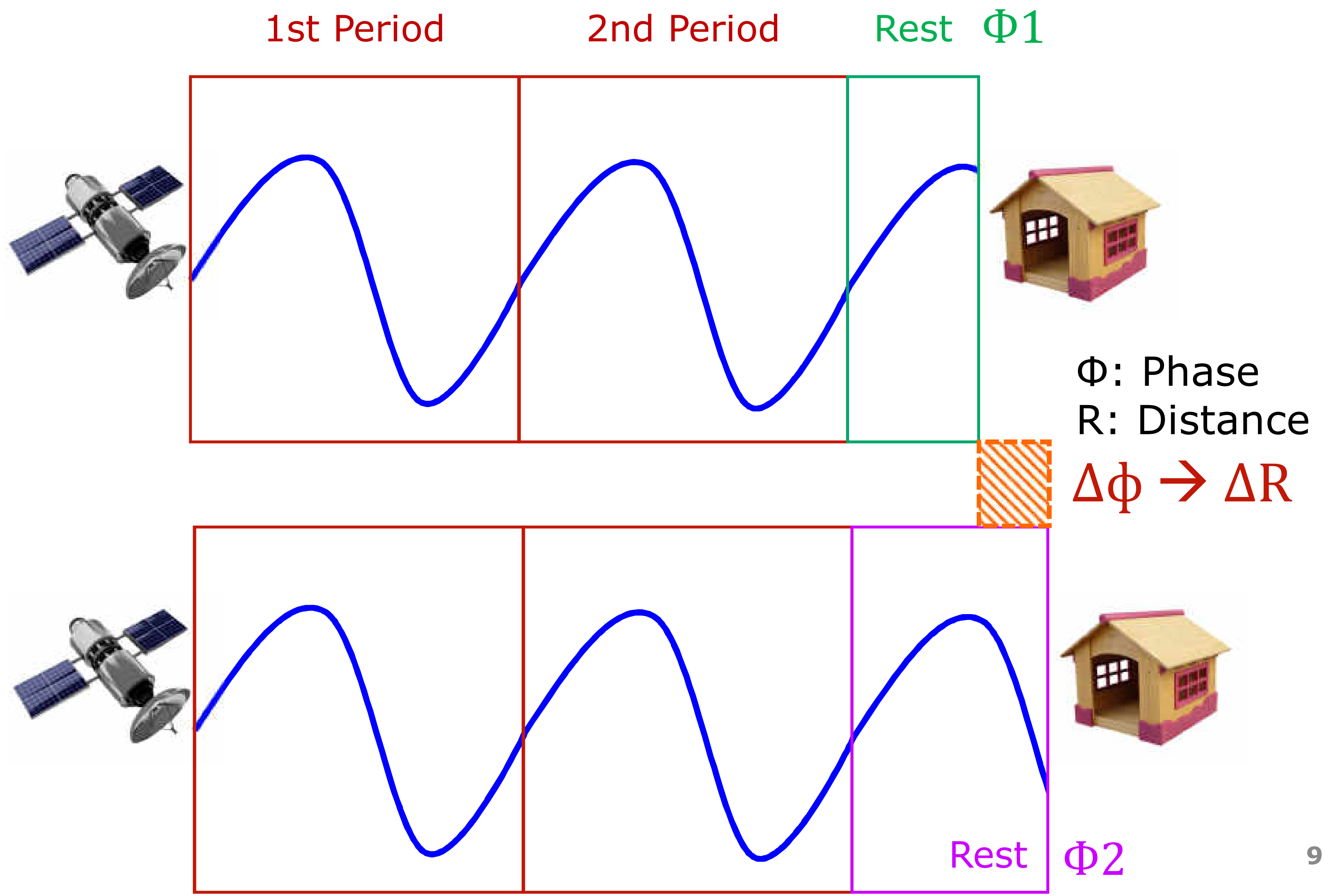

Phase Difference

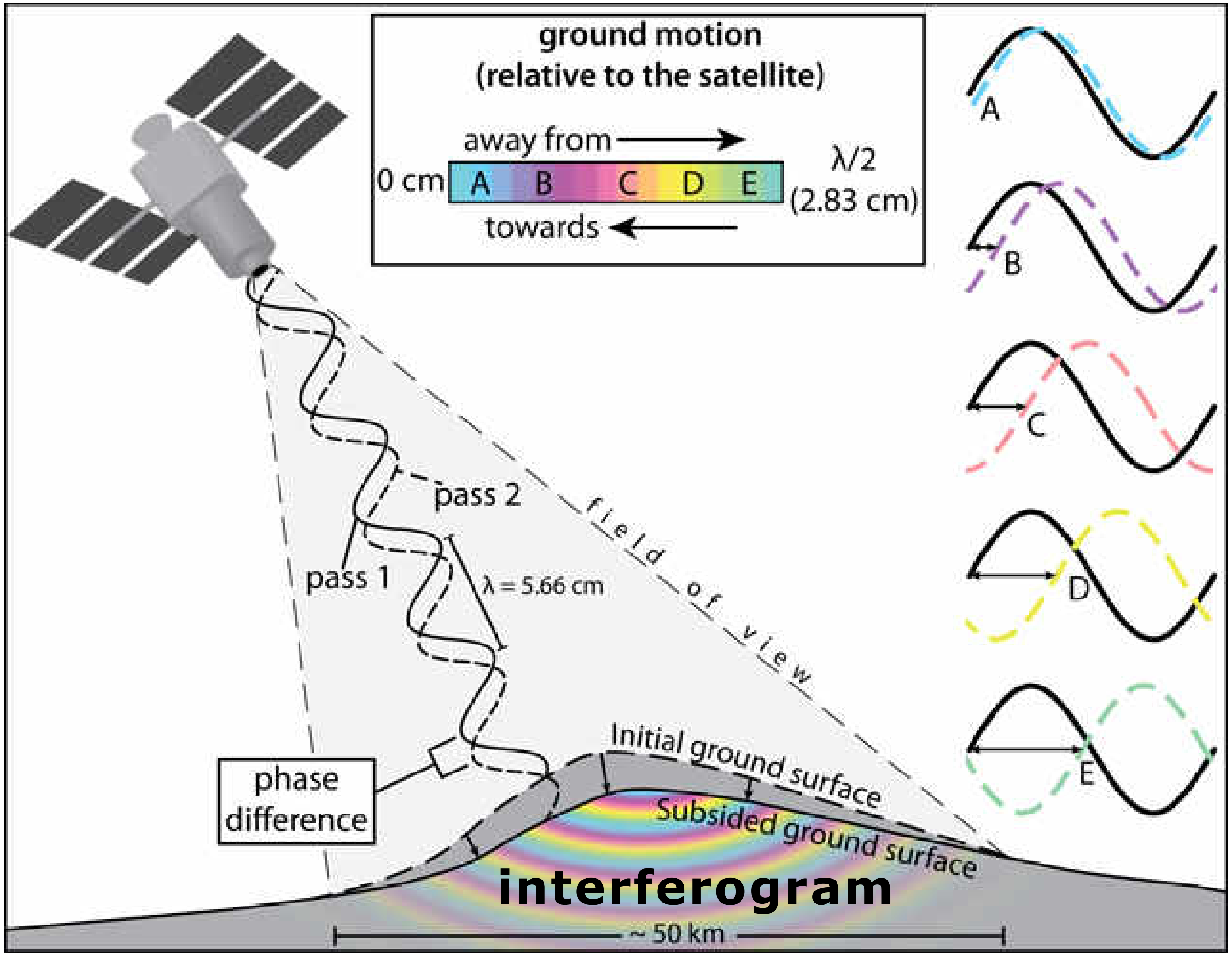

SAR Interferometry (InSAR)

The interferometric phase contains some distinct contributions:

$$\varphi_{\text{int}} = \varphi_f + \varphi_{topo} + \varphi_{displ} + \varphi_{atm} + \varphi_{err}$$

φ_f	flat Earth
φ_{topo}	topographic phase
φ_{displ}	deformation phase
φ_{atm}	atmospheric phase
φ_{err}	noise (error phase)

Phase Difference

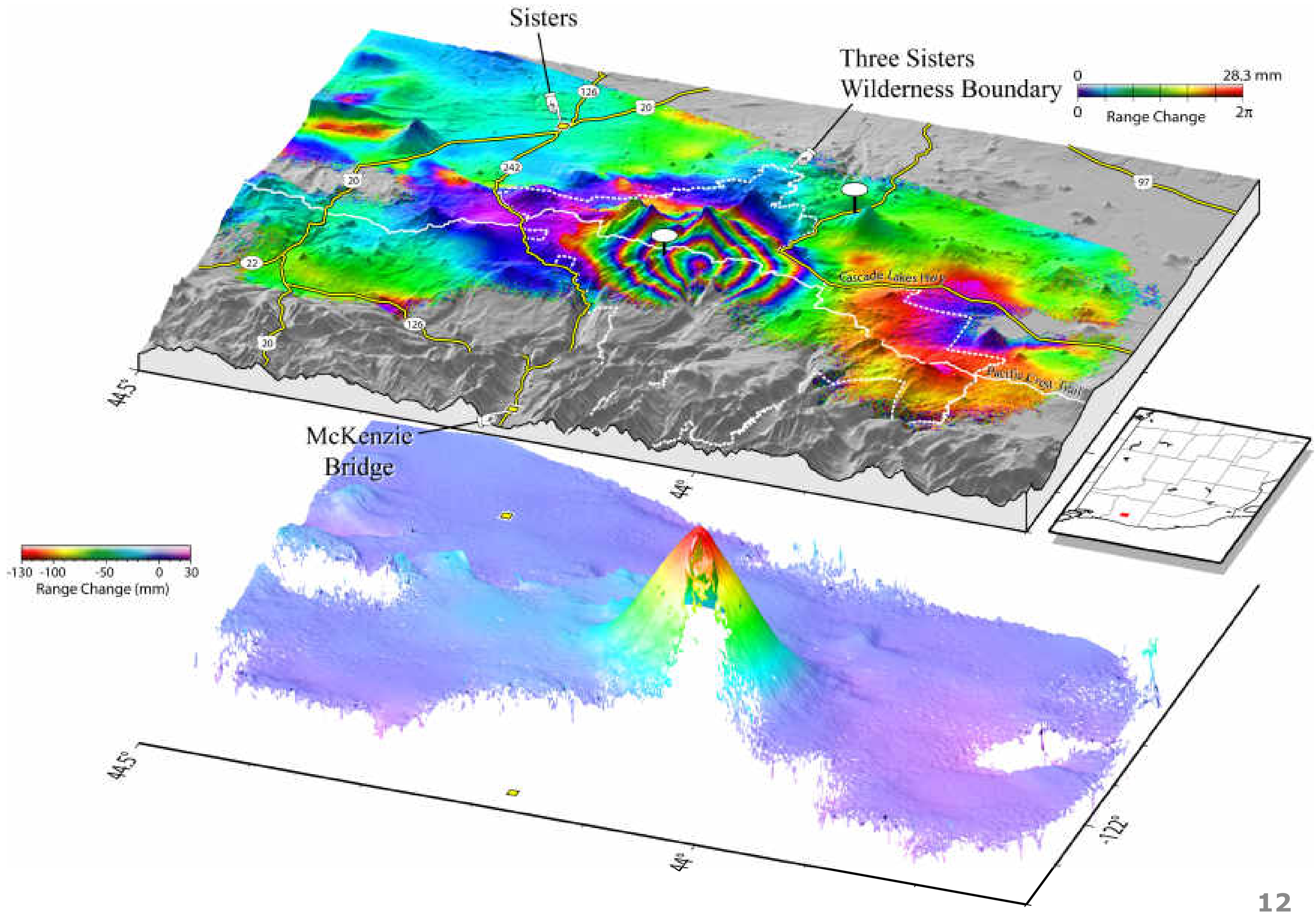

PS – Persistent Scatterers

Pixels that are highly correlated in backscattered amplitude and phase

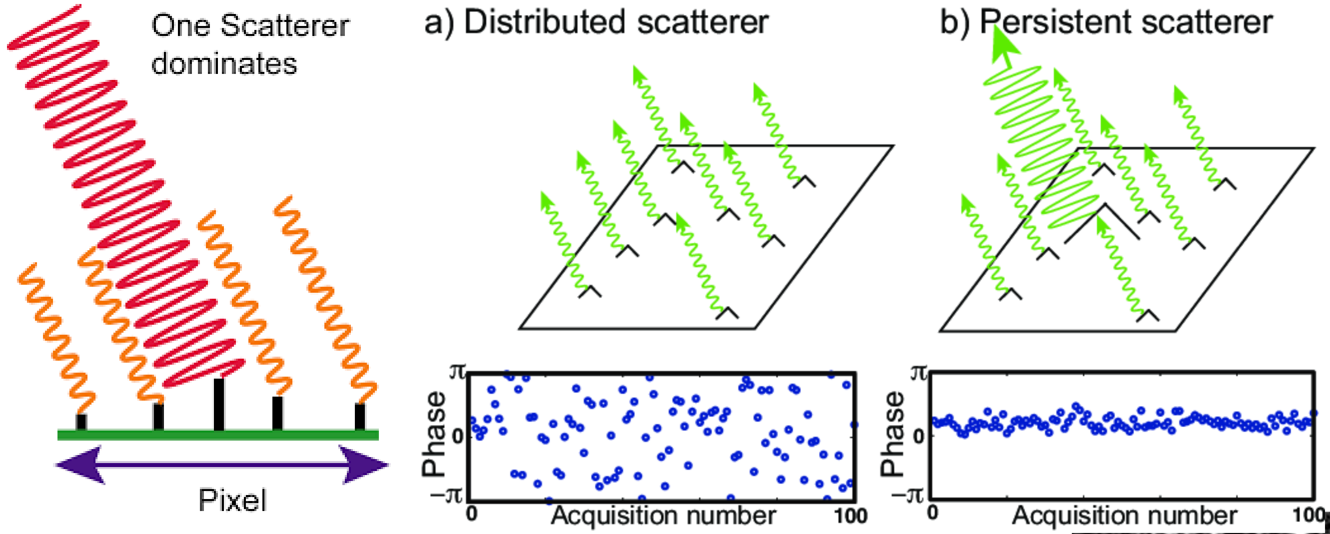

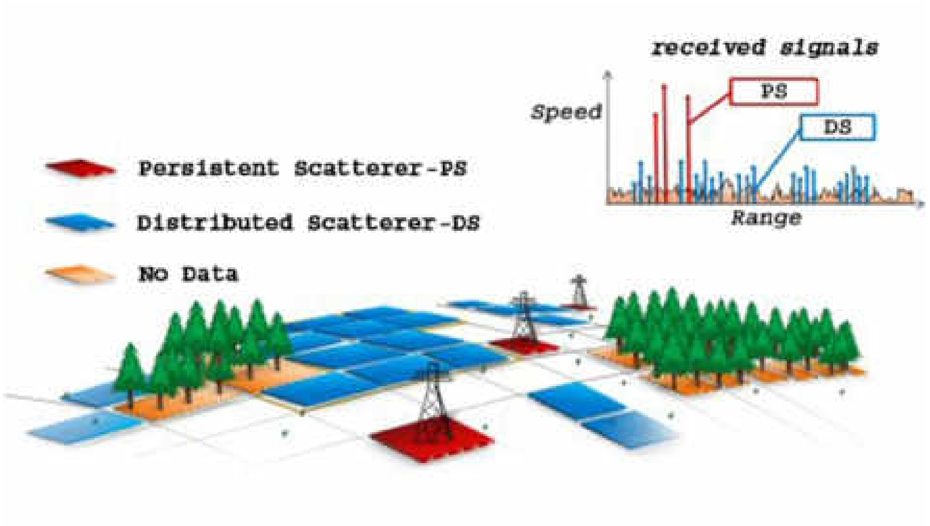

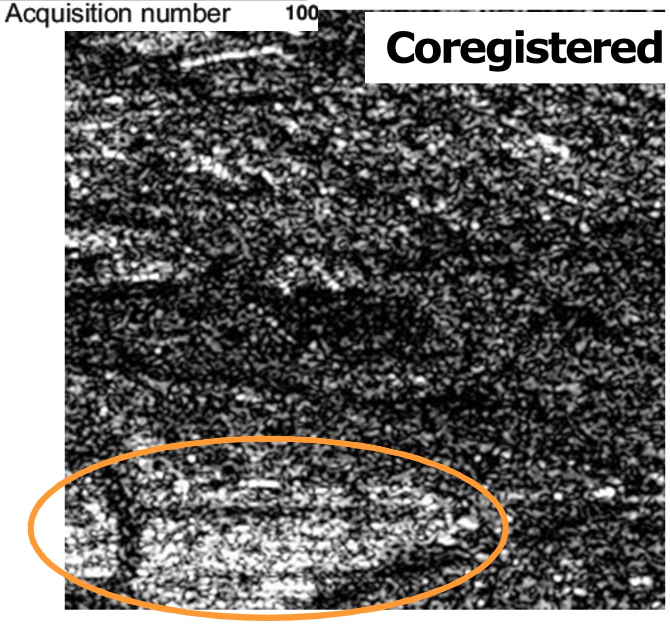

SBAS – Small Baseline Subset

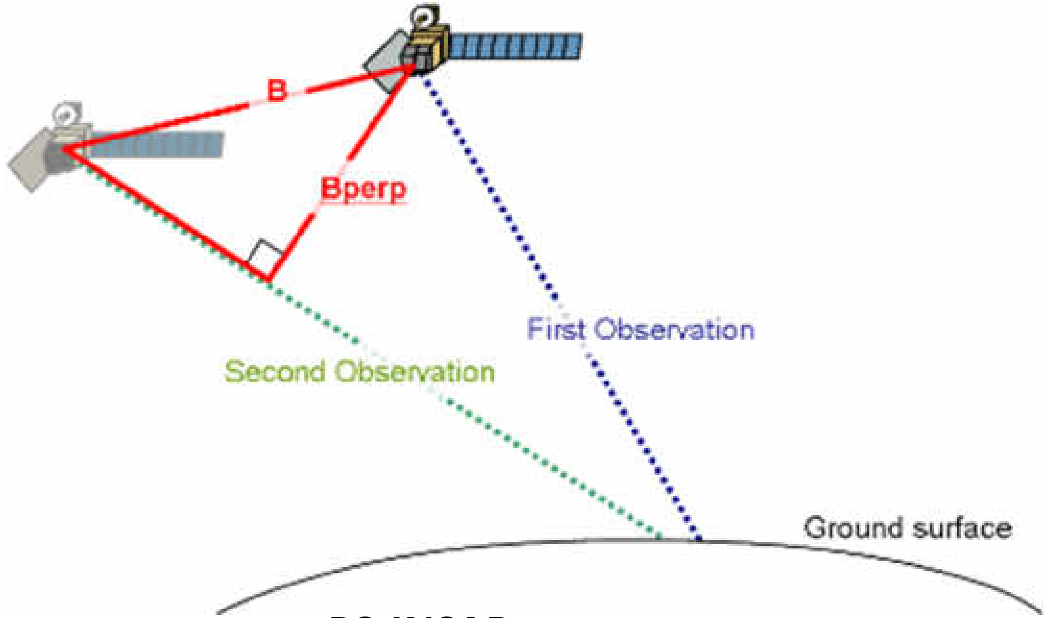

Ideal case: $\beta_{perp} = 0$

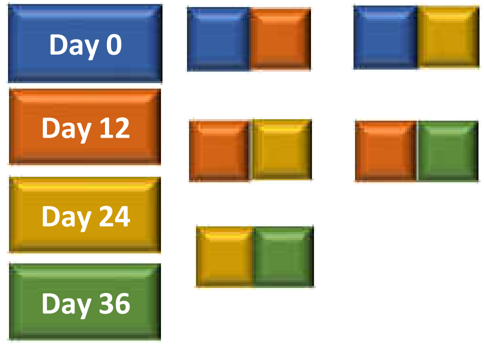

Acquisition Date between two images < 25 days

PS-INSAR

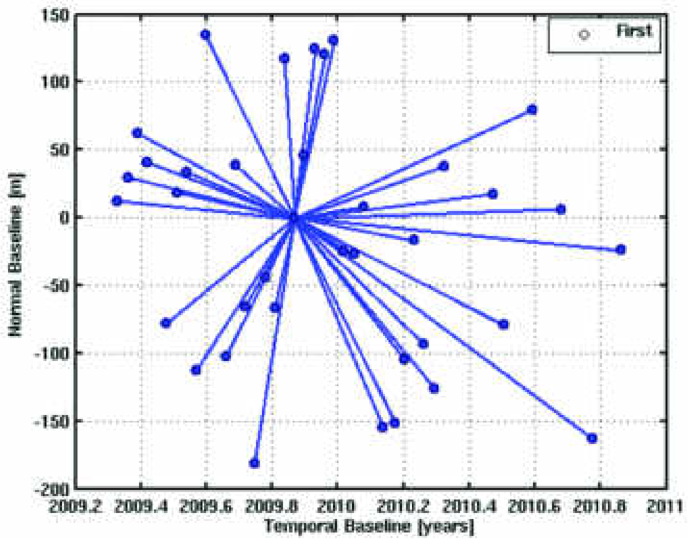

SBAS-INSAR

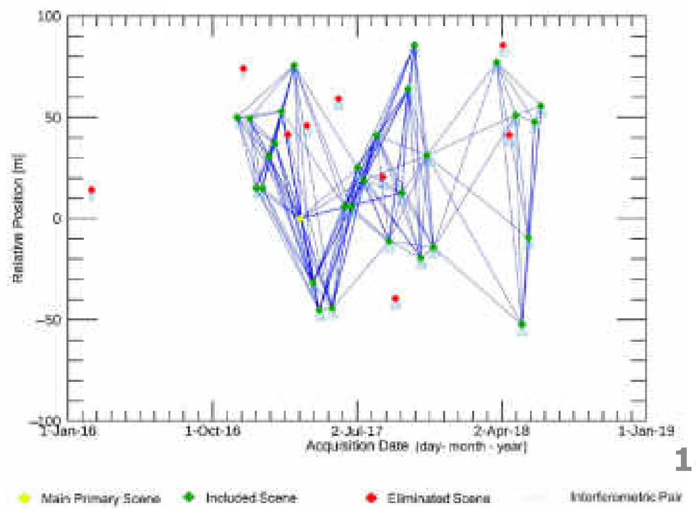

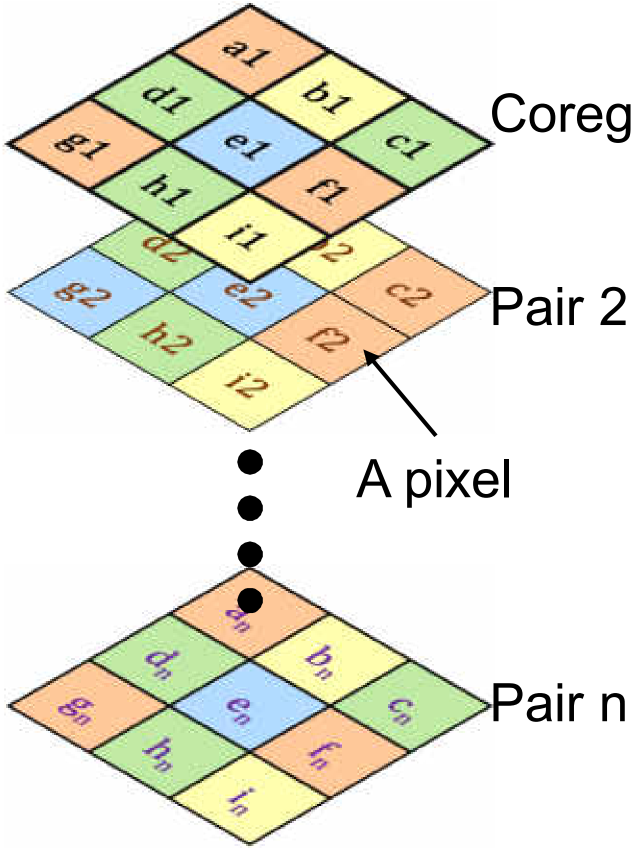

$$m_a = \frac{1}{k}\sum_{k=1}^{n} a_k$$

$$\sigma_a = \sqrt{\frac{1}{k}\sum_{k=1}^{n}(a_k - m_a)}$$

PERSISTENT SCATTERER EXTRACTION

$$D_A = \frac{\sigma_A}{m_A}$$

D_A : Amplitude Dispersion Index

σ_A: St.Dev of amplitude values

m_A: Mean of amplitude values

$$\boldsymbol{D_A \le 0.3}$$

Data set

Table 1: Sentinel-1 data information

	Sentinel-1A	Sentinel-1B
Orbit direction	Ascending	
Product Type	Single Look Complex (SLC), Interferometric Wide swath (IW) mode	
Path	69	69
Frame	74	73
Incidence Angle (degree)	$31^{o} – 46^{o}$	
Heading Angle (degree)	$347.6\ ^{o}$	
Azimuth resolution (m)	20	
Range resolution (m)	5	
Polarization	VV+VH	
Number of images	287	
Acquisition Period	14th April 2016 – 28th October 2022	

Workflow Summary

1. **Image Pair Selection:**
   - Maximum num. of image pairs
   - Avoid temporal and spatial decorrelation
2. **Noise phase removal**
3. **Select stable scattering pixels** by:
   - High average phase coherence
   - Low amplitude dispersion index

$$D_A = \frac{\sigma_{amp.}}{\mu_{amp..}}$$

4. **Phase unwrapping** to get displacements at stable pixels
5. **Calibrate** raw displacements by GPS data

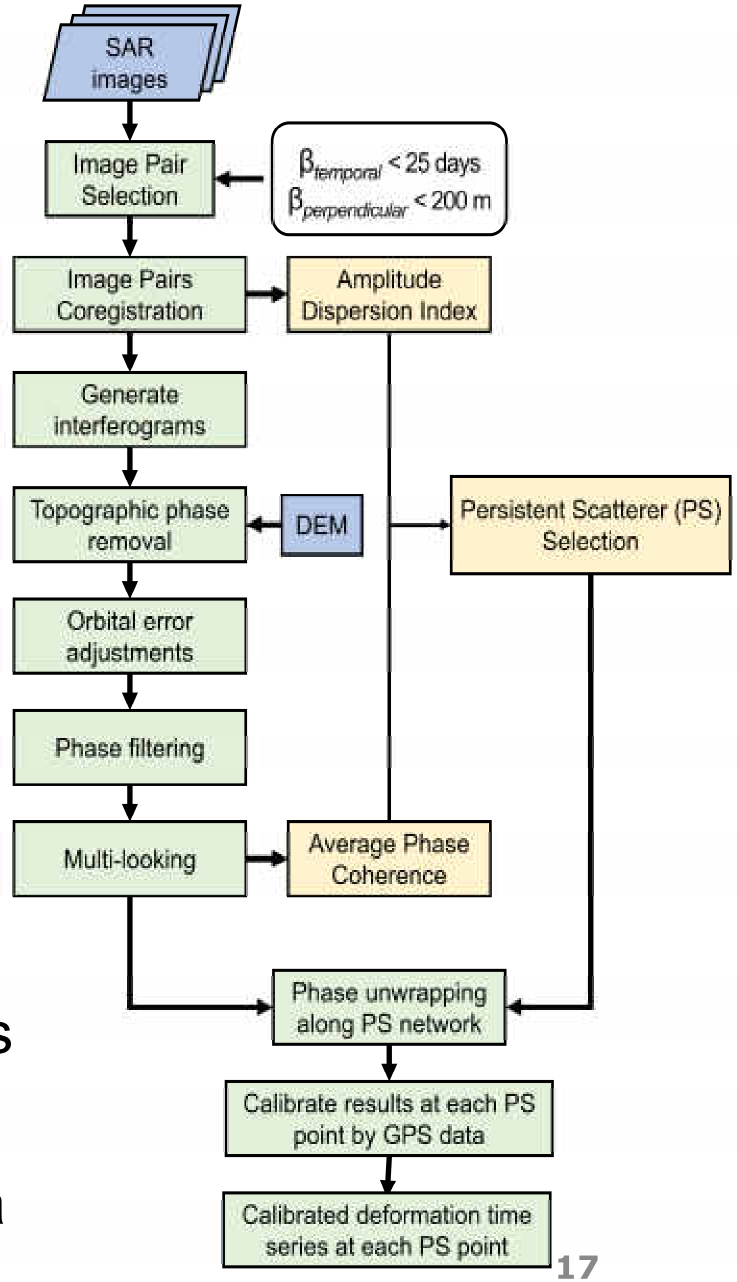

Why calibrated by GPS instead of leveling?

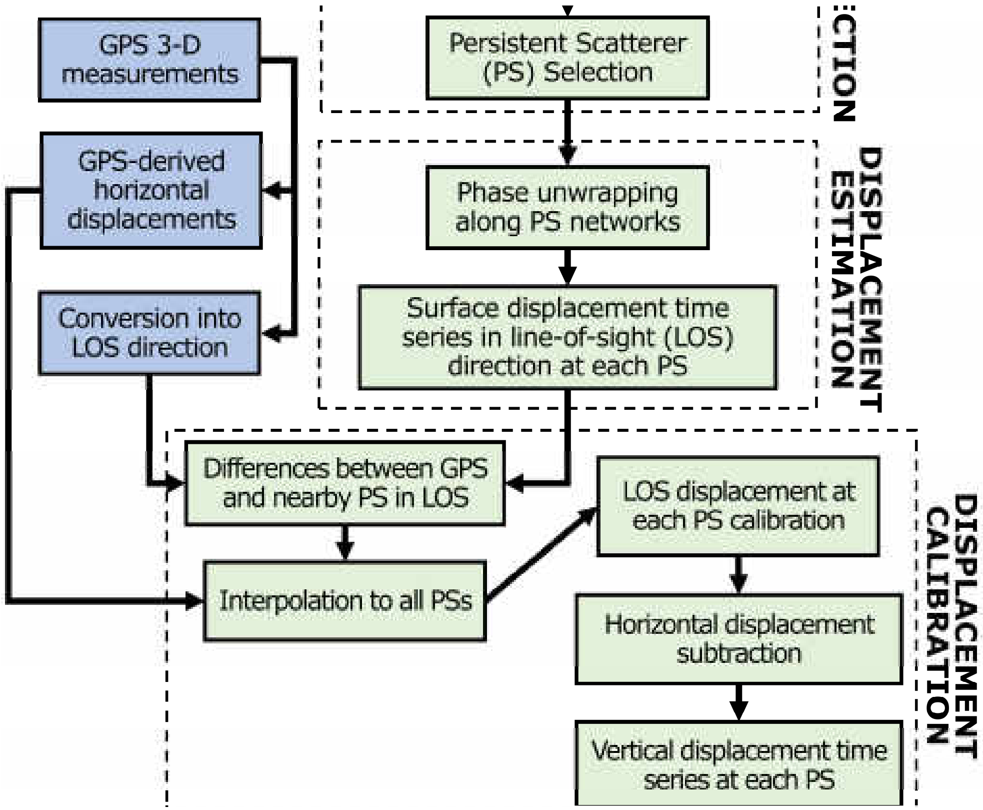

Validation by Leveling

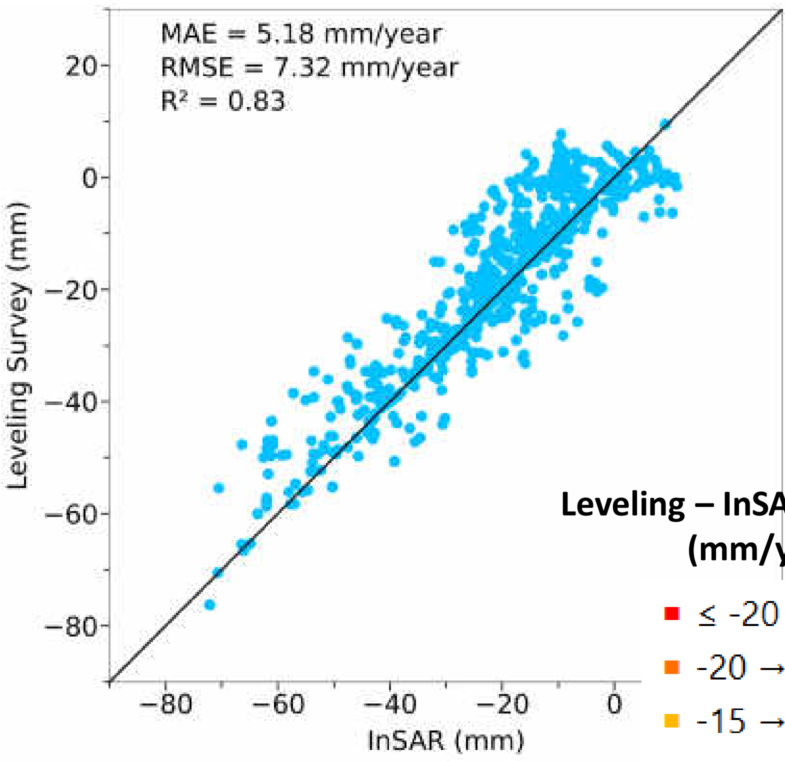

Leveling – InSAR Difference (mm/year)

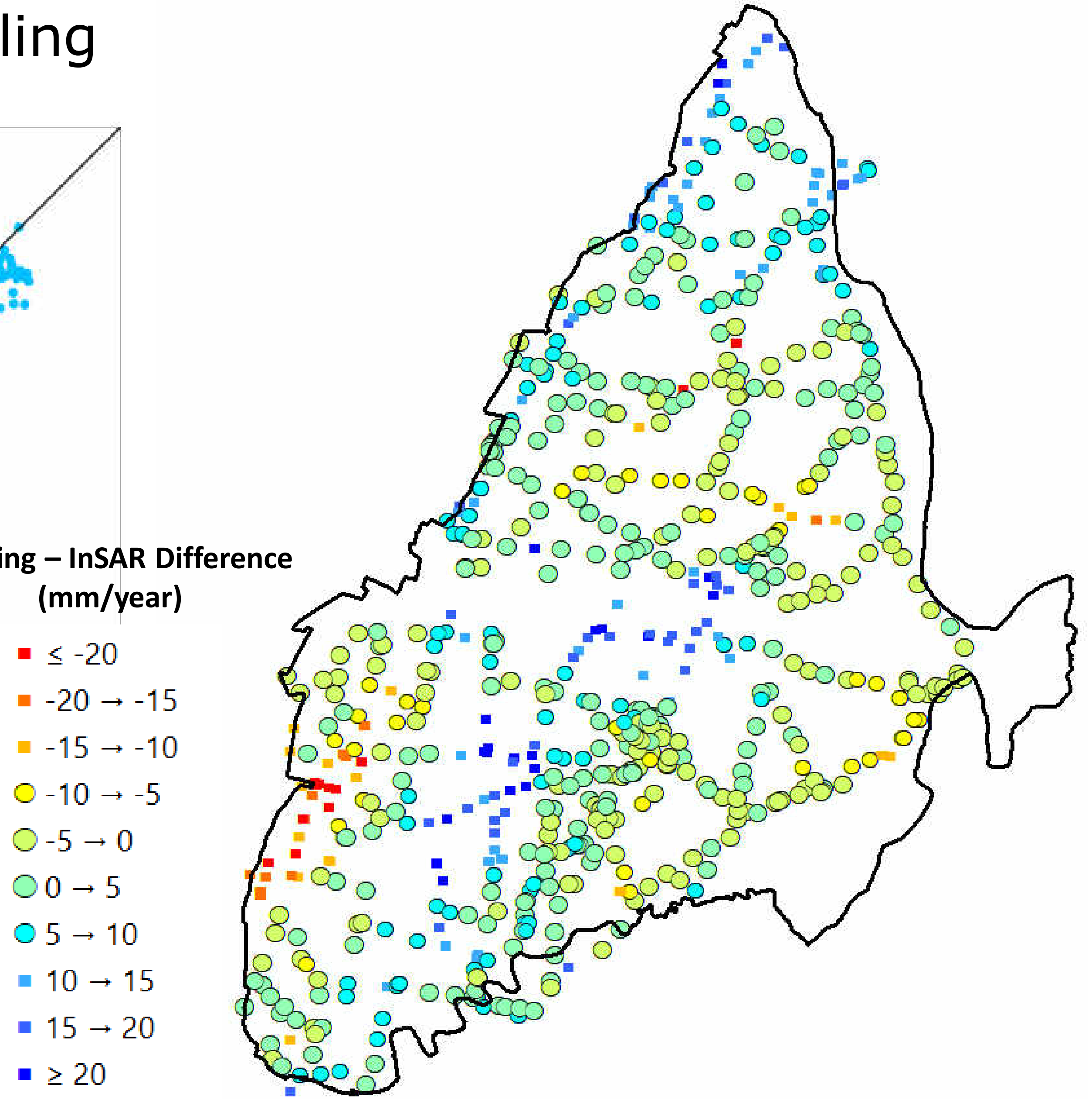

Validation by Leveling

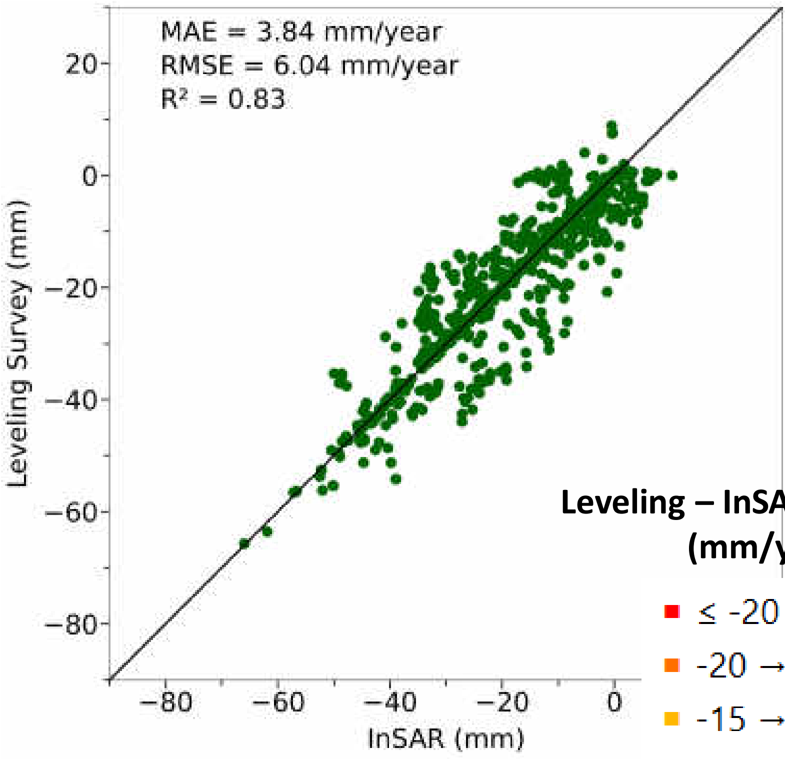

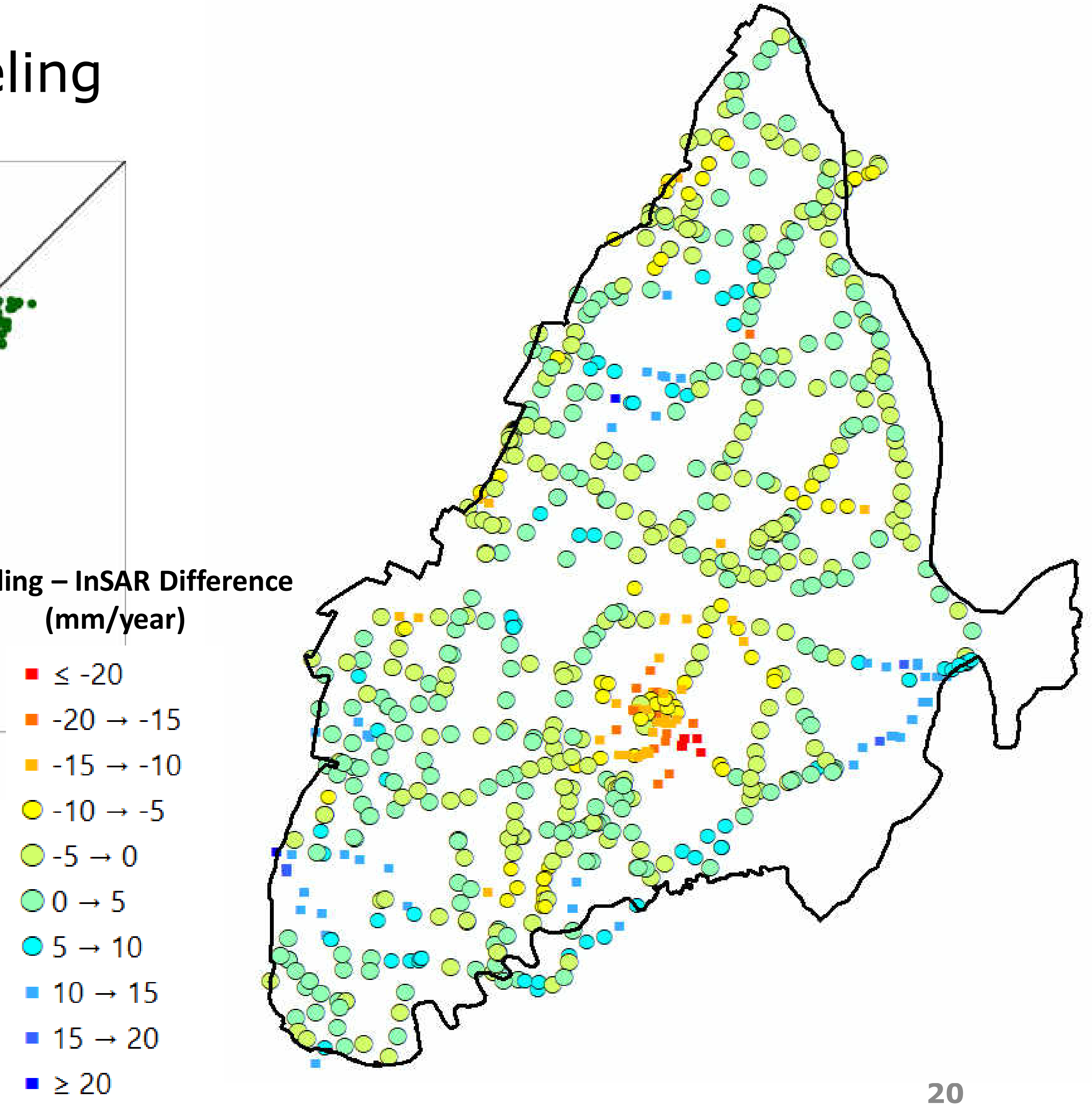

Validation by Leveling

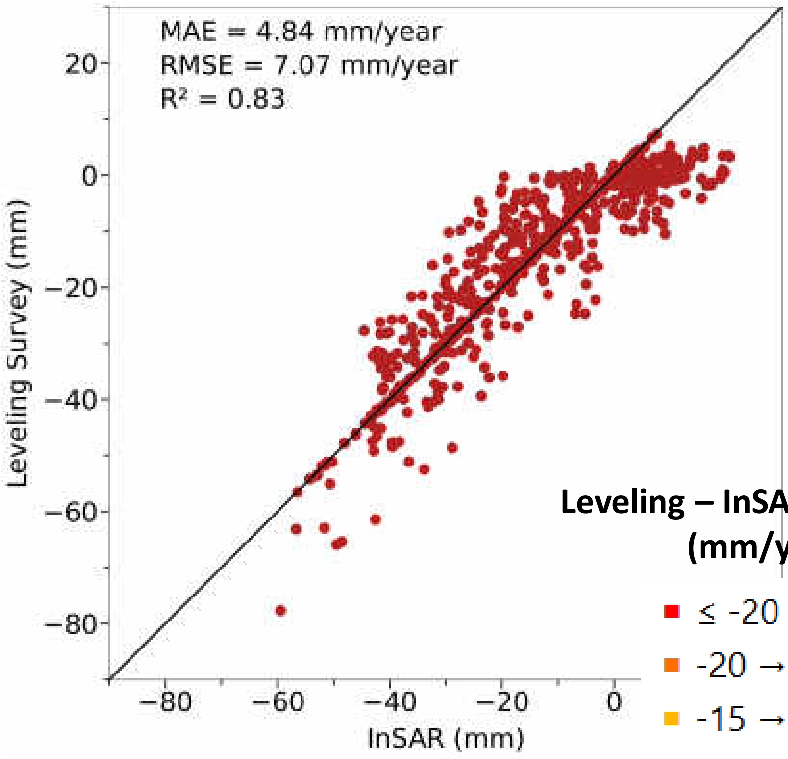

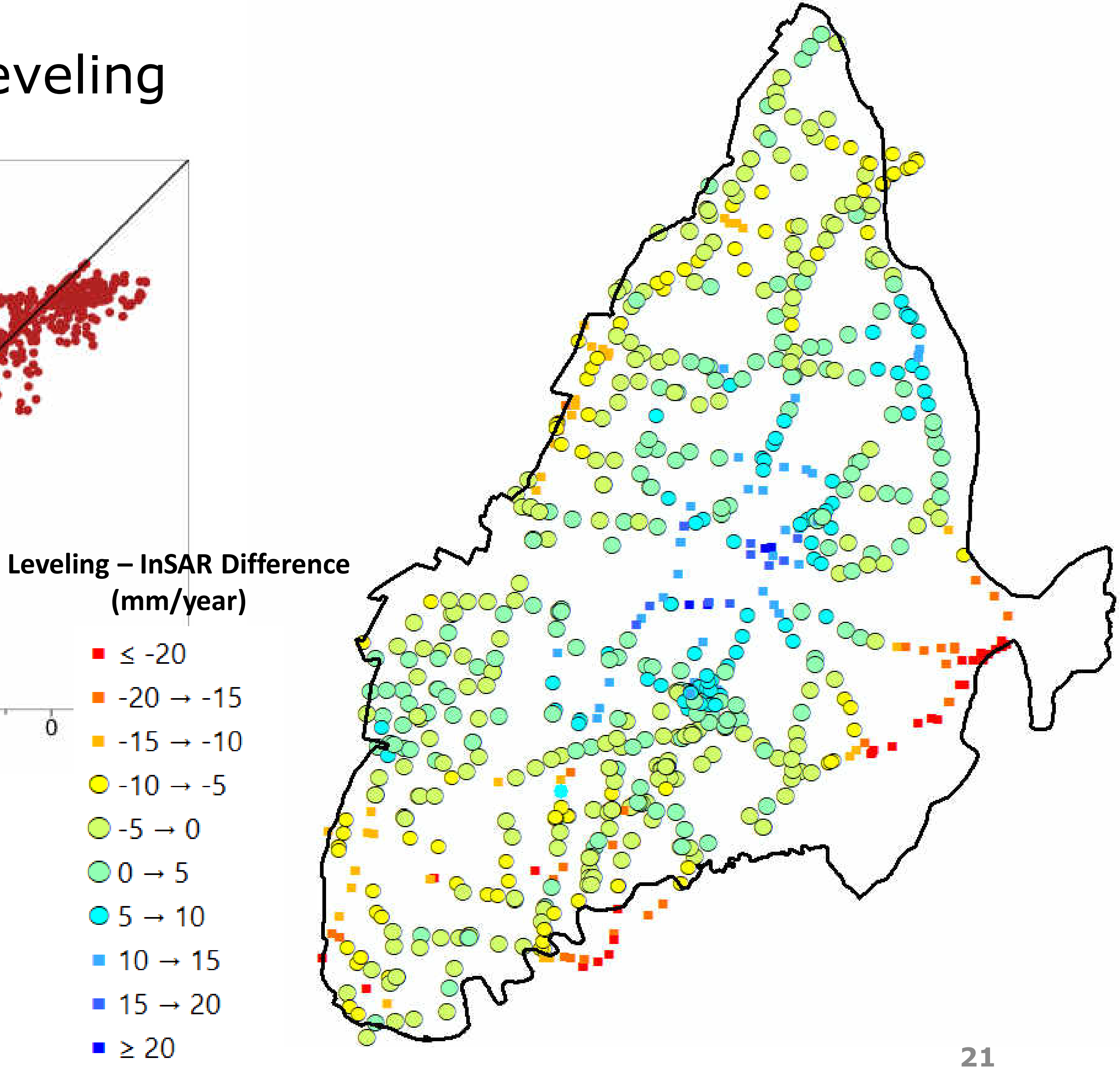

Validation by Leveling (near THSR railway)

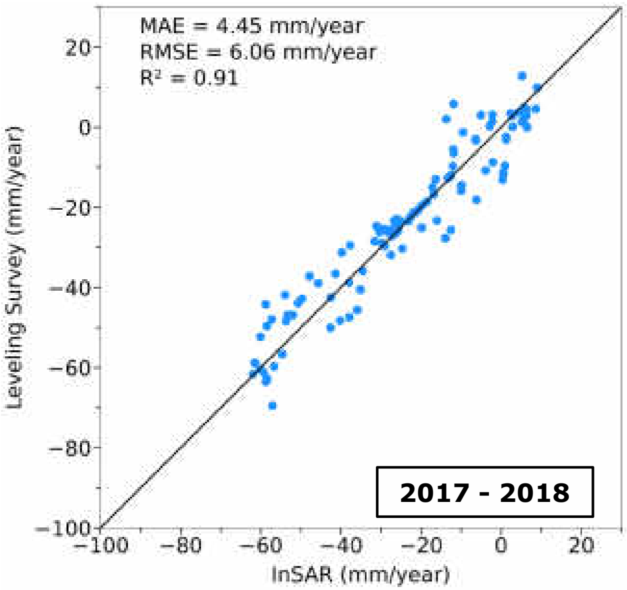

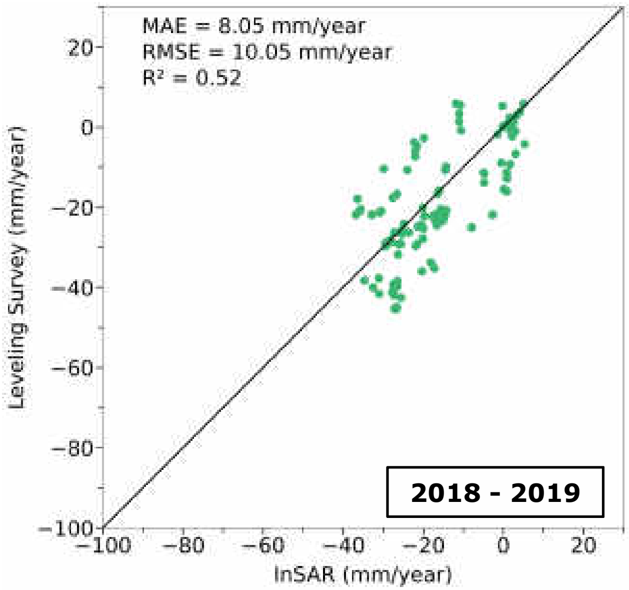

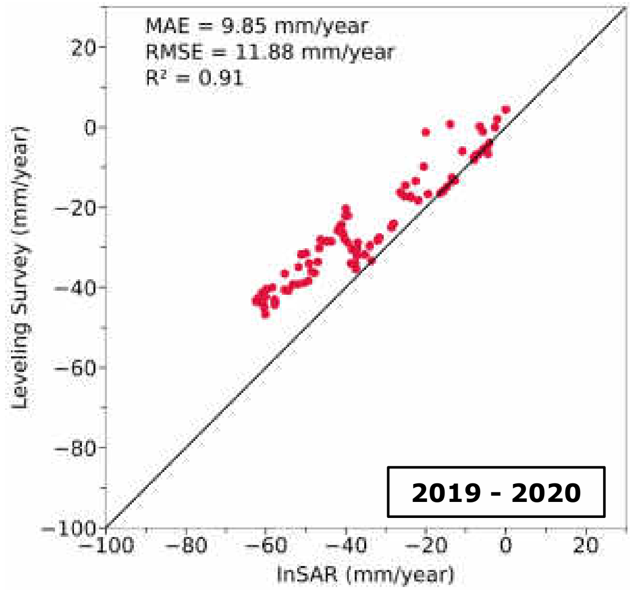

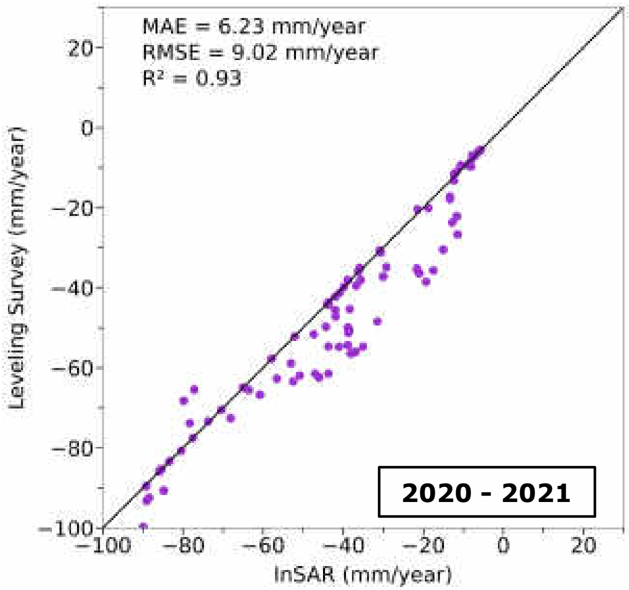

Cumulative deformation map

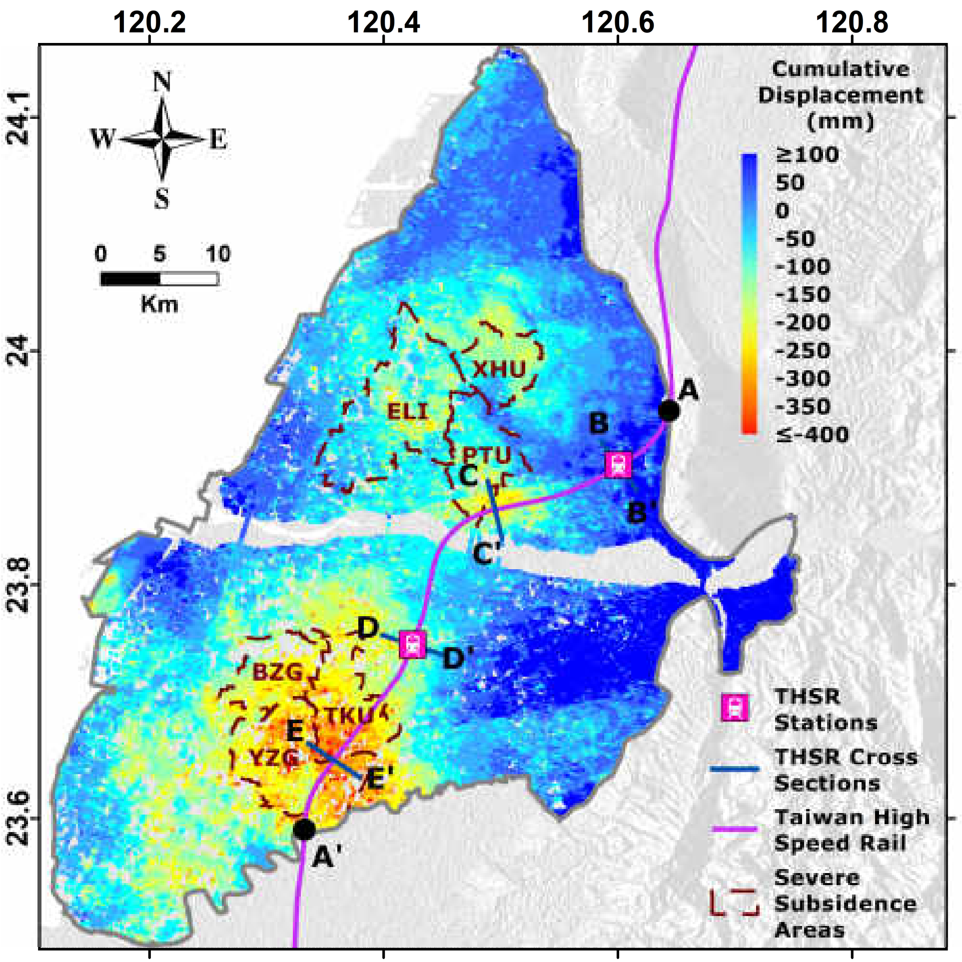

Average Velocity

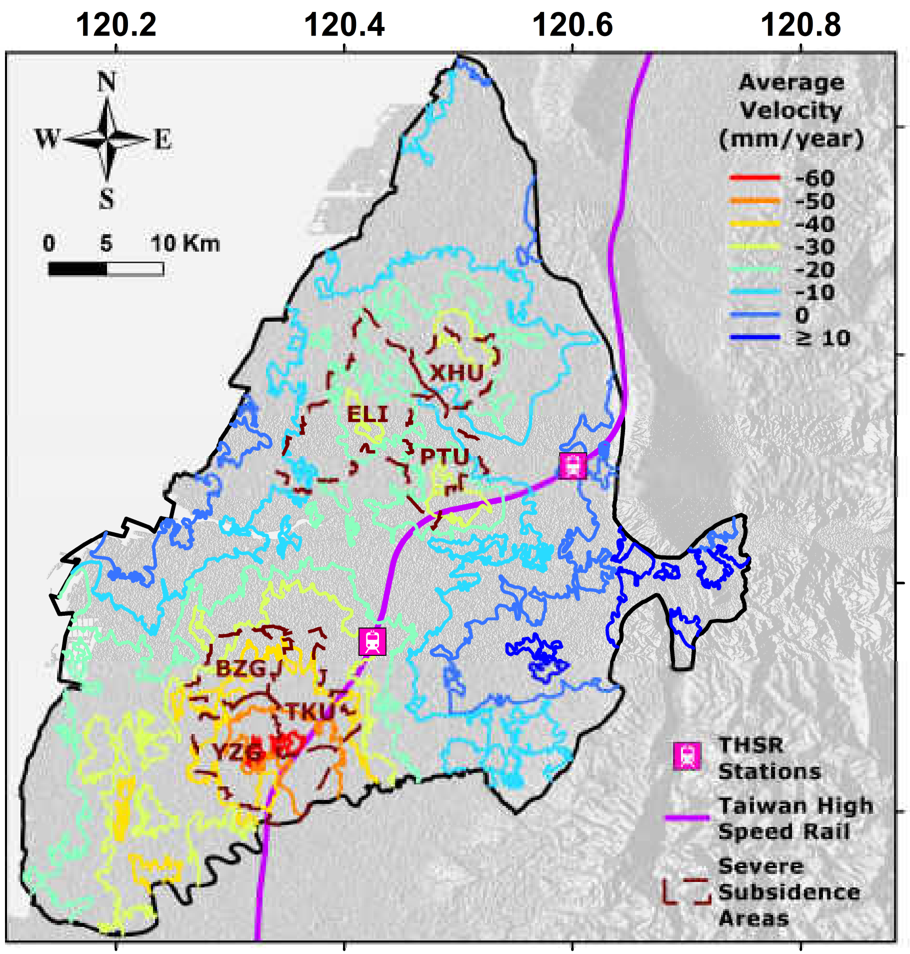

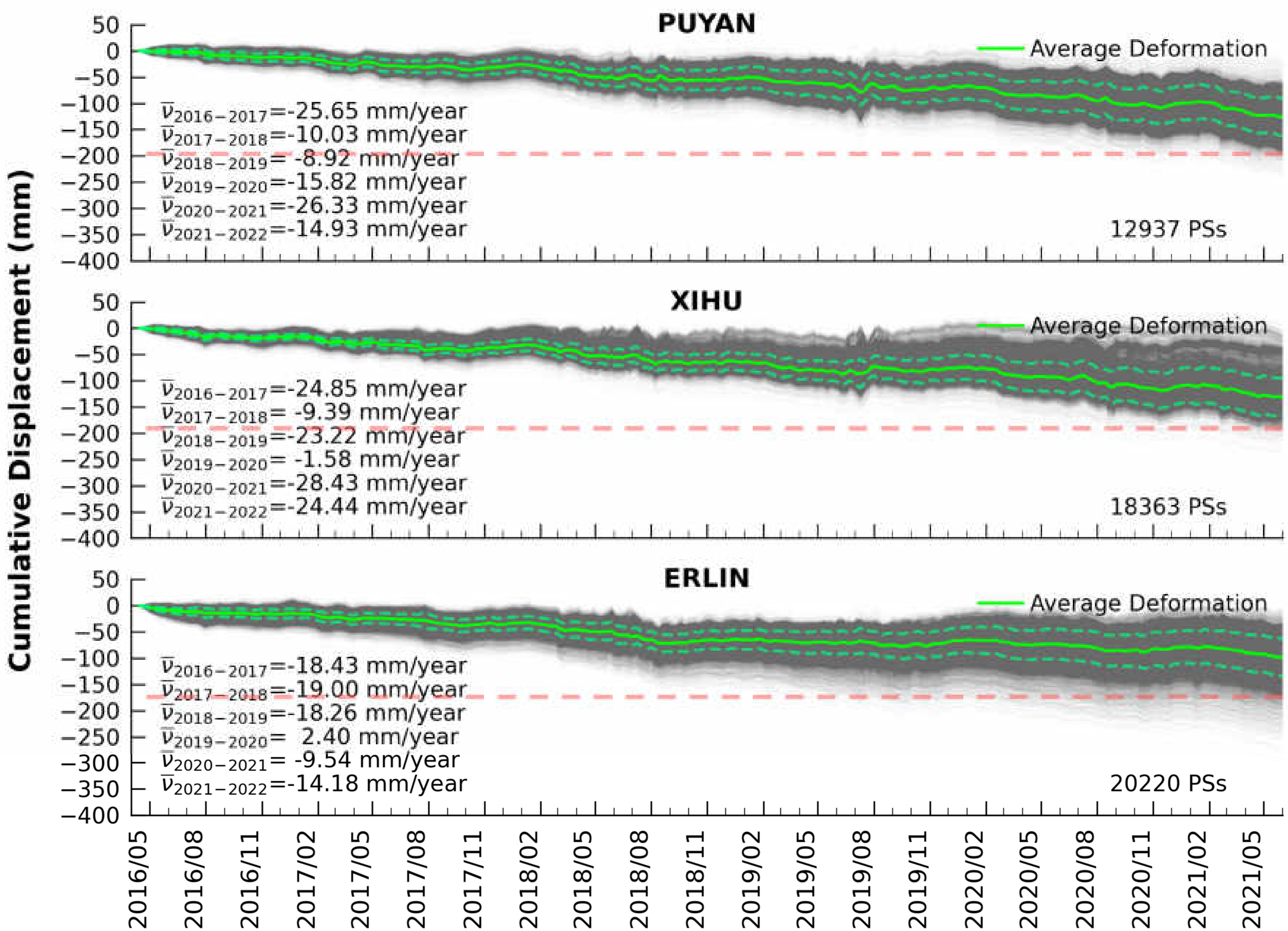
Cumulative Displacement (mm)
PUYAN
Average Deformation
$\overline{v}_{2016-2017}$=-25.65 mm/year
$\overline{v}_{2017-2018}$=-10.03 mm/year
$\overline{v}_{2018-2019}$= -8.92 mm/year
$\overline{v}_{2019-2020}$=-15.82 mm/year
$\overline{v}_{2020-2021}$=-26.33 mm/year
$\overline{v}_{2021-2022}$=-14.93 mm/year
12937 PSs
XIHU
Average Deformation
$\overline{v}_{2016-2017}$=-24.85 mm/year
$\overline{v}_{2017-2018}$= -9.39 mm/year
$\overline{v}_{2018-2019}$=-23.22 mm/year
$\overline{v}_{2019-2020}$= -1.58 mm/year
$\overline{v}_{2020-2021}$=-28.43 mm/year
$\overline{v}_{2021-2022}$=-24.44 mm/year
18363 PSs
ERLIN
Average Deformation
$\overline{v}_{2016-2017}$=-18.43 mm/year
$\overline{v}_{2017-2018}$=-19.00 mm/year
$\overline{v}_{2018-2019}$=-18.26 mm/year
$\overline{v}_{2019-2020}$= 2.40 mm/year
$\overline{v}_{2020-2021}$= -9.54 mm/year
$\overline{v}_{2021-2022}$=-14.18 mm/year
20220 PSs
50
0
−50
−100
−150
−200
−250
−300
−350
−400
2016/05
2016/08
2016/11
2017/02
2017/05
2017/08
2017/11
2018/02
2018/05
2018/08
2018/11
2019/02
2019/05
2019/08
2019/11
2020/02
2020/05
2020/08
2020/11
2021/02
2021/05

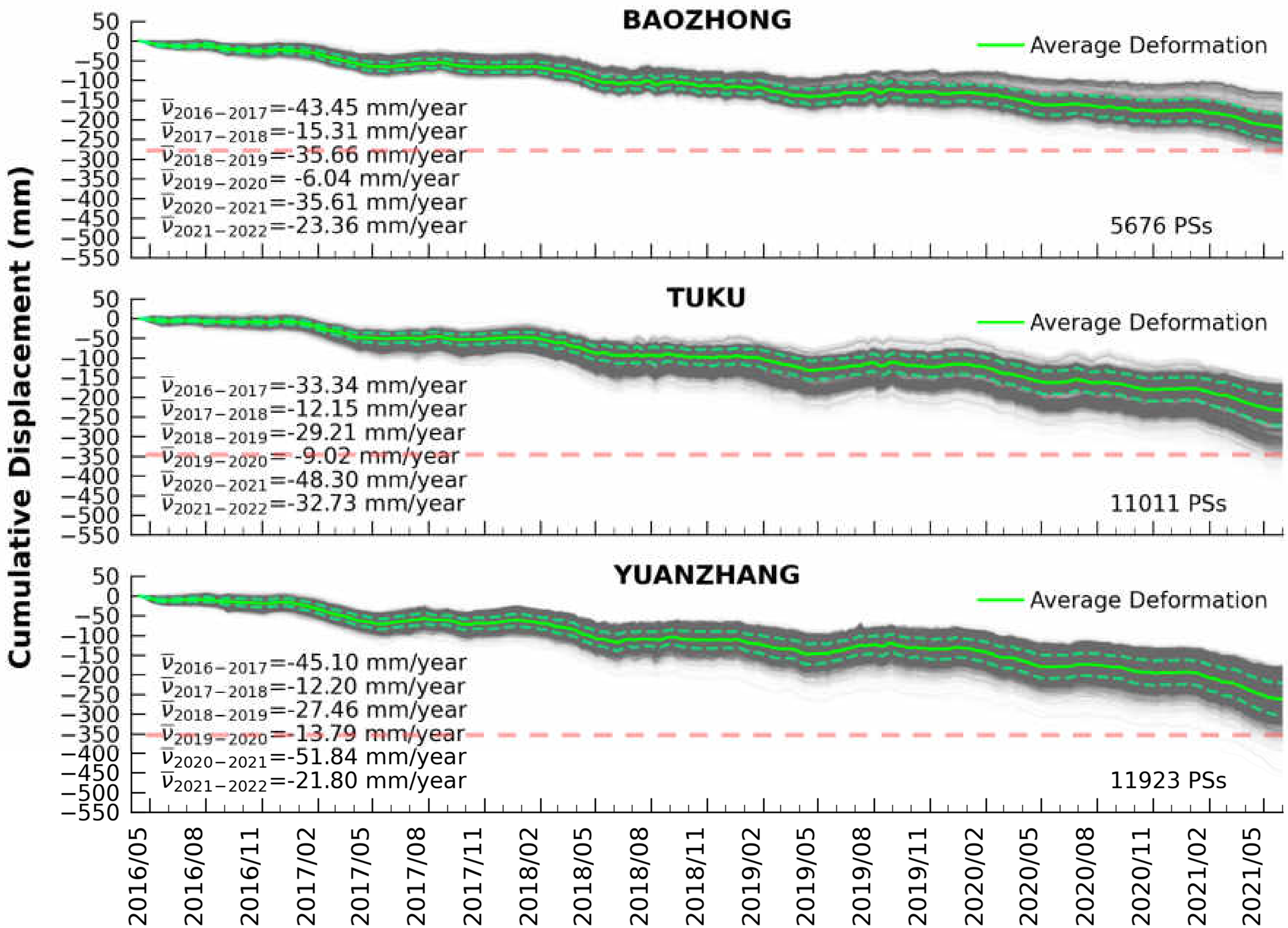
BAOZHONG
Average Deformation
$\bar{v}_{2016-2017}$=-43.45 mm/year
$\bar{v}_{2017-2018}$=-15.31 mm/year
$\bar{v}_{2018-2019}$=-35.66 mm/year
$\bar{v}_{2019-2020}$= -6.04 mm/year
$\bar{v}_{2020-2021}$=-35.61 mm/year
$\bar{v}_{2021-2022}$=-23.36 mm/year
5676 PSs
TUKU
Average Deformation
$\bar{v}_{2016-2017}$=-33.34 mm/year
$\bar{v}_{2017-2018}$=-12.15 mm/year
$\bar{v}_{2018-2019}$=-29.21 mm/year
$\bar{v}_{2019-2020}$= -9.02 mm/year
$\bar{v}_{2020-2021}$=-48.30 mm/year
$\bar{v}_{2021-2022}$=-32.73 mm/year
11011 PSs
YUANZHANG
Average Deformation
$\bar{v}_{2016-2017}$=-45.10 mm/year
$\bar{v}_{2017-2018}$=-12.20 mm/year
$\bar{v}_{2018-2019}$=-27.46 mm/year
$\bar{v}_{2019-2020}$=-13.79 mm/year
$\bar{v}_{2020-2021}$=-51.84 mm/year
$\bar{v}_{2021-2022}$=-21.80 mm/year
11923 PSs
Cumulative Displacement (mm)
50
0
−50
−100
−150
−200
−250
−300
−350
−400
−450
−500
−550
2016/05
2016/08
2016/11
2017/02
2017/05
2017/08
2017/11
2018/02
2018/05
2018/08
2018/11
2019/02
2019/05
2019/08
2019/11
2020/02
2020/05
2020/08
2020/11
2021/02
2021/05

Cumulative subsidence along THSR

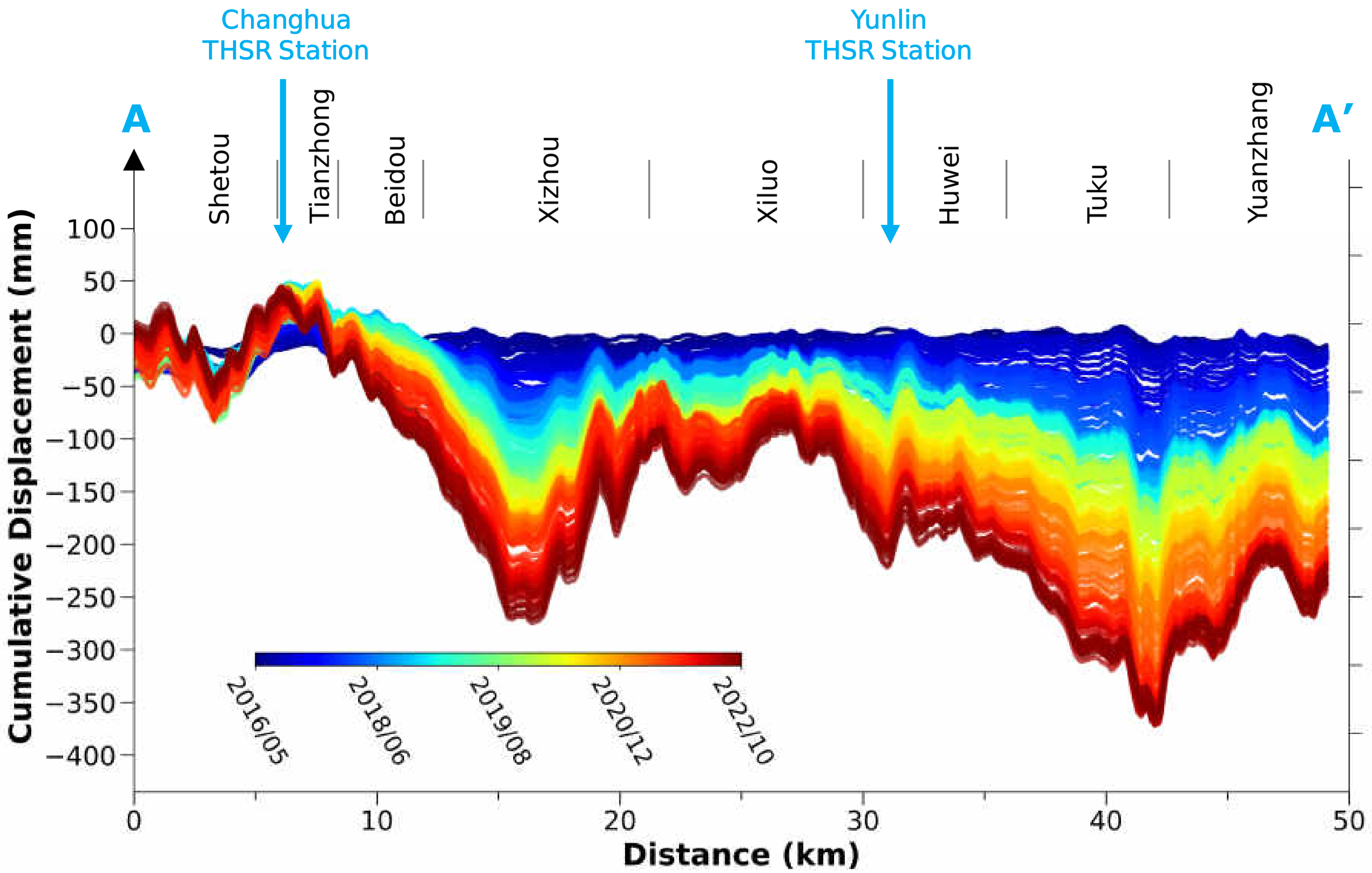

Cumulative subsidence across THSR

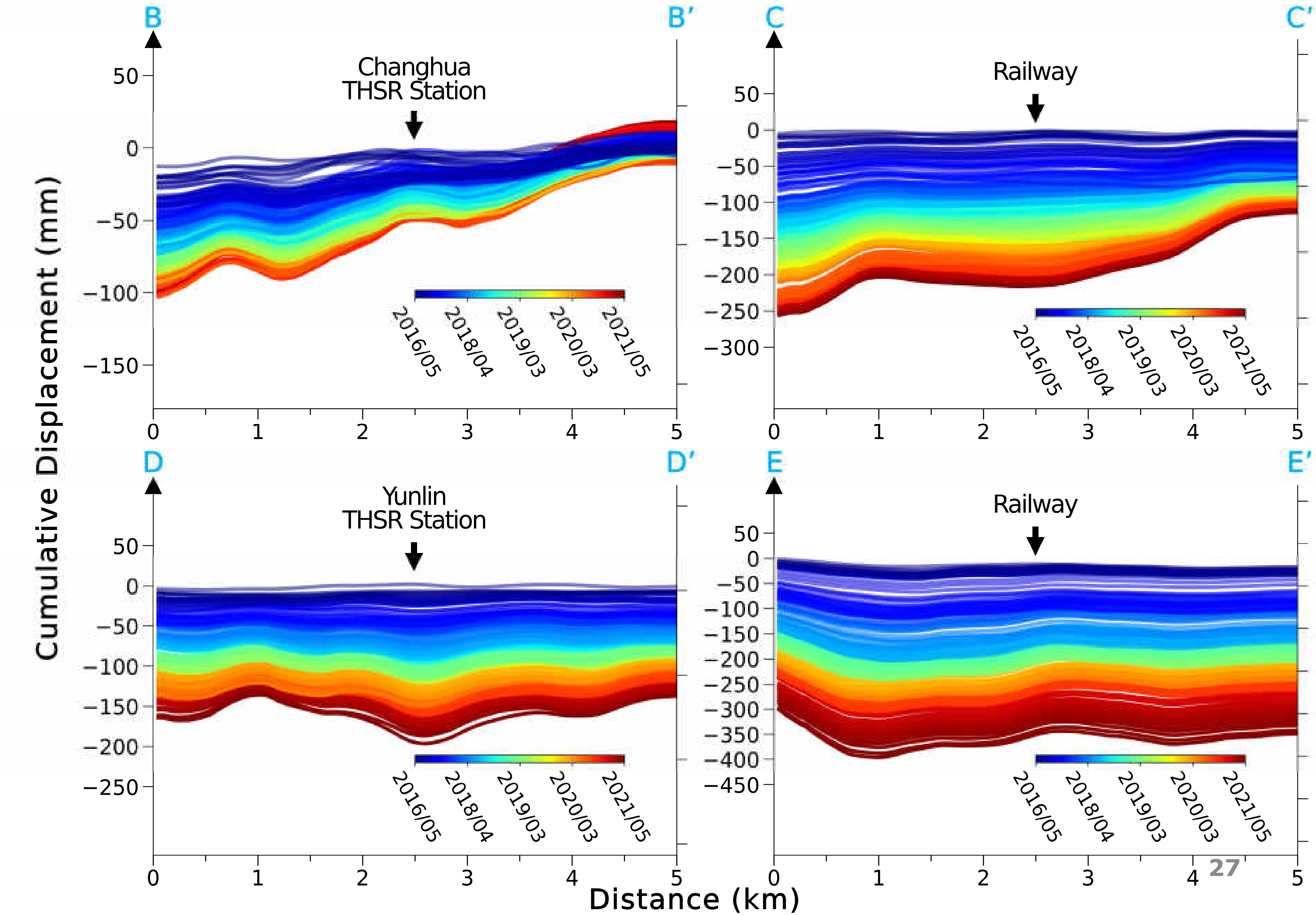

- Apply SBAS-PSInSAR method to analyze 287 Sentinel-1's SAR images
- Monitoring land subsidence development in CRFP (2016 – 2022)
- Results calibrated by GPS and validated by leveling survey

- Three subsidence bowls in **Changhua**, c.disp. up to -25 cm; average velocity -2 → -4 cm/year
- A huge subsidence bowl in **Yunlin**, c.disp. Reach -40 cm; average velocity -3 → -6 cm/year
- Deformation time-series show stronger variations in Yunlin
- Subsidence THSR profiles indicate 3 serious subsidence locations, average velocity -3 → -6 cm/year
- Subsidence velocity accelerate in 2020 – 2021


THANK YOU
FOR YOUR
ATTENTION

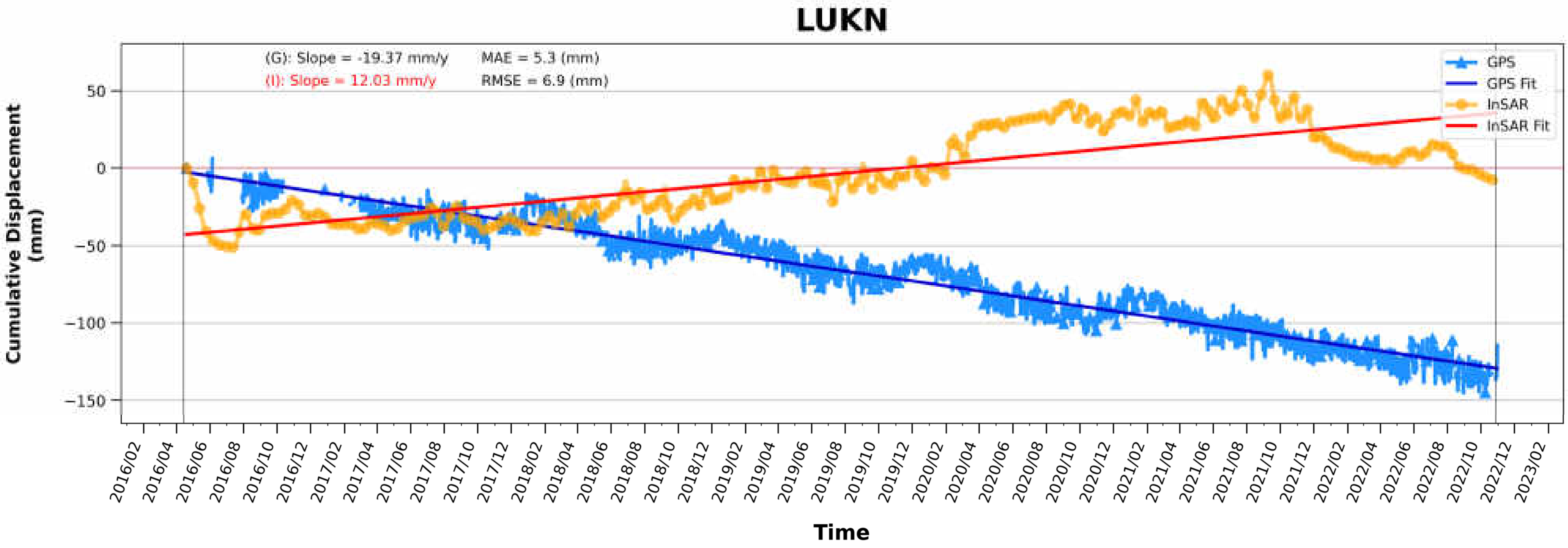
LUKN
(G): Slope = -19.37 mm/y
MAE = 5.3 (mm)
(I): Slope = 12.03 mm/y
RMSE = 6.9 (mm)
GPS
GPS Fit
InSAR
InSAR Fit
Cumulative Displacement (mm)
Time

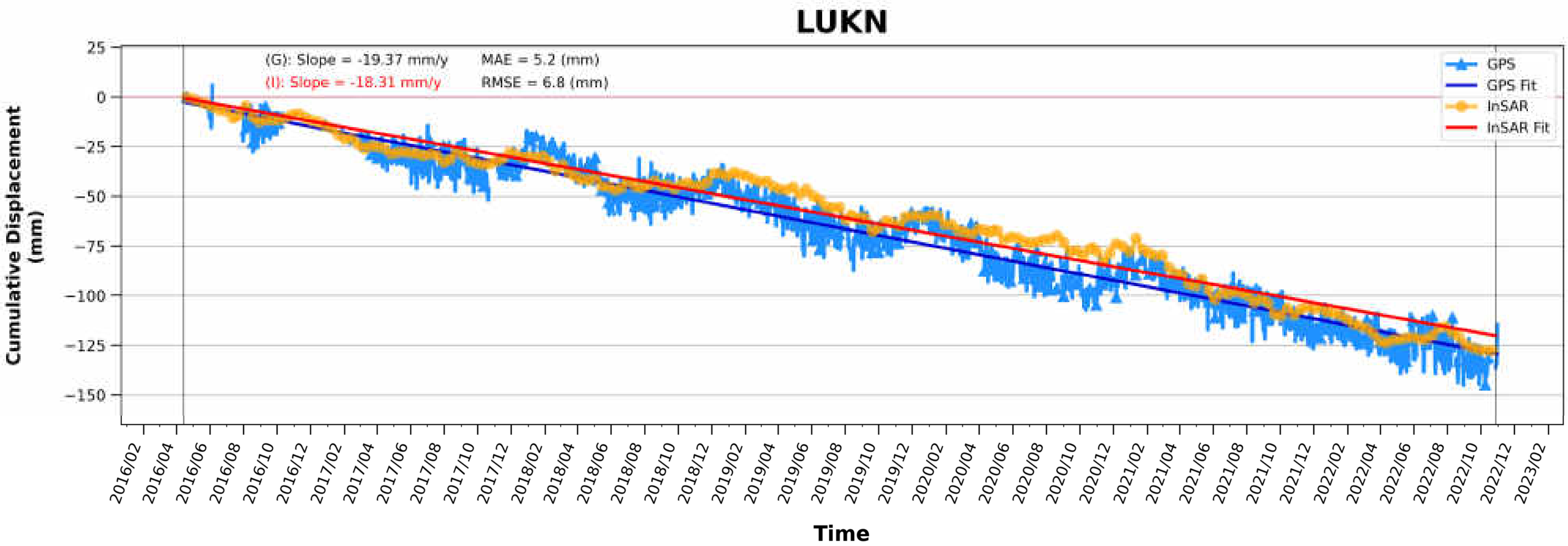
LUKN
(G): Slope = -19.37 mm/y
MAE = 5.2 (mm)
(I): Slope = -18.31 mm/y
RMSE = 6.8 (mm)
GPS
GPS Fit
InSAR
InSAR Fit
Cumulative Displacement (mm)
Time

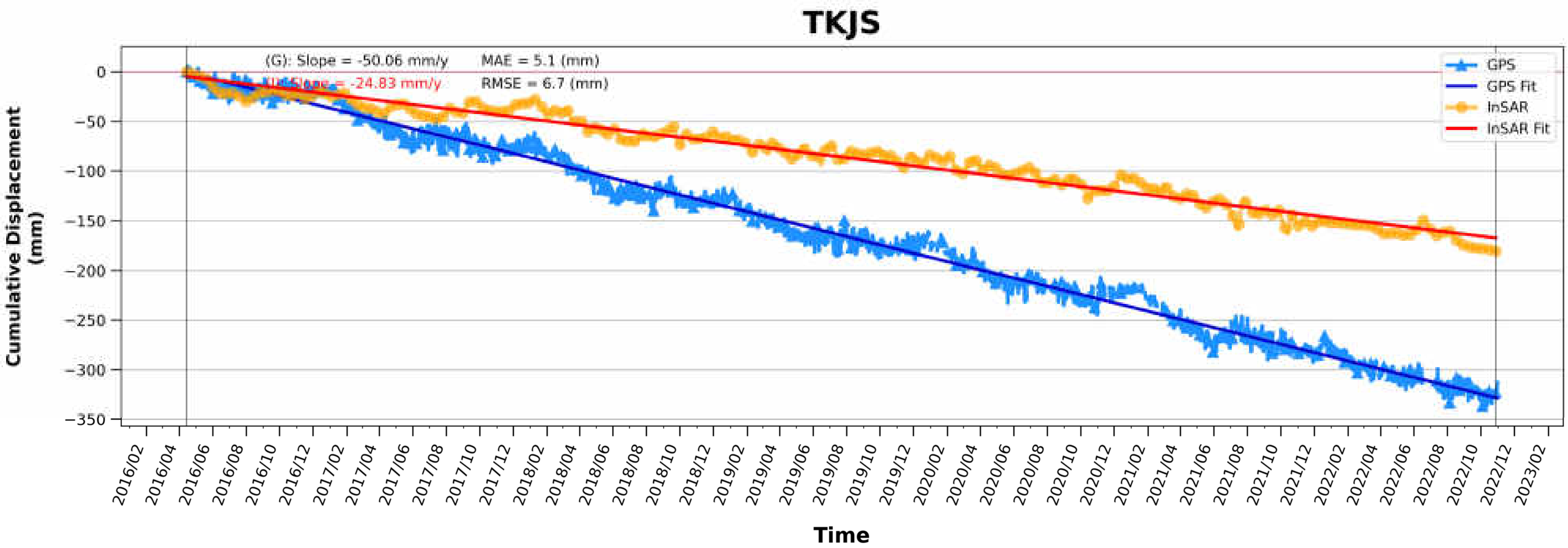
TKJS
(G): Slope = -50.06 mm/y
Slope = -24.83 mm/y
MAE = 5.1 (mm)
RMSE = 6.7 (mm)
GPS
GPS Fit
InSAR
InSAR Fit
Cumulative Displacement (mm)
Time

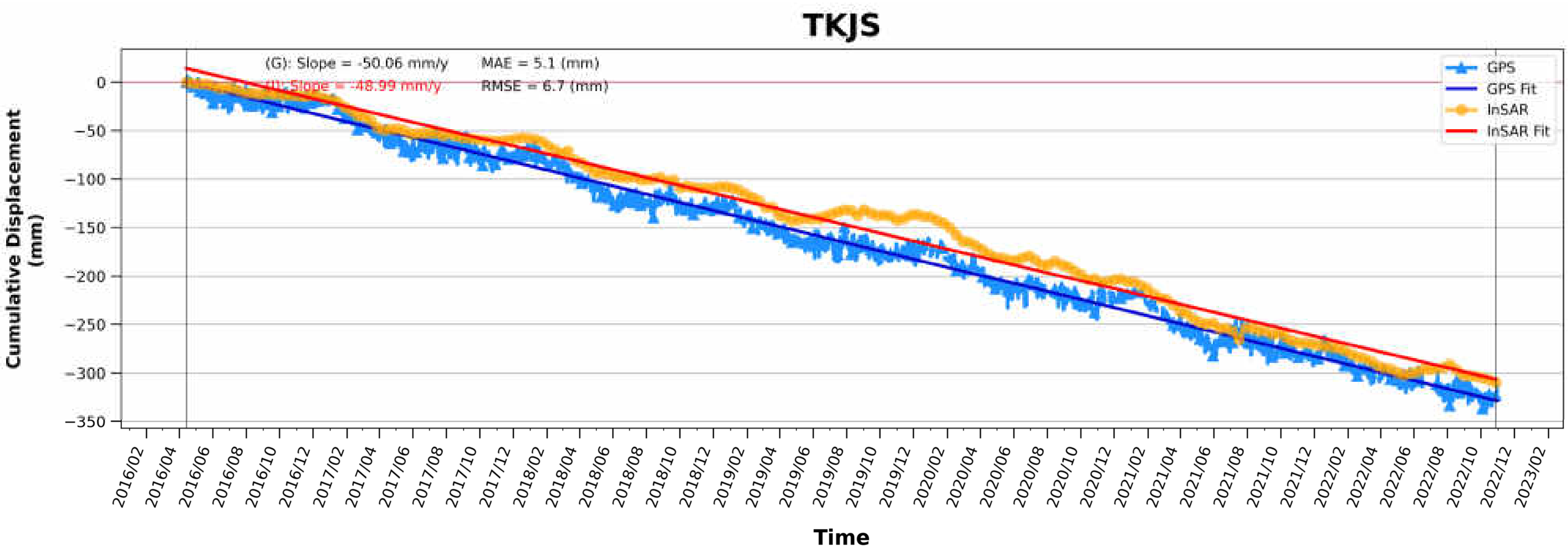
TKJS
(G): Slope = -50.06 mm/y
Slope = -48.99 mm/y
MAE = 5.1 (mm)
RMSE = 6.7 (mm)
GPS
GPS Fit
InSAR
InSAR Fit
Cumulative Displacement (mm)
Time

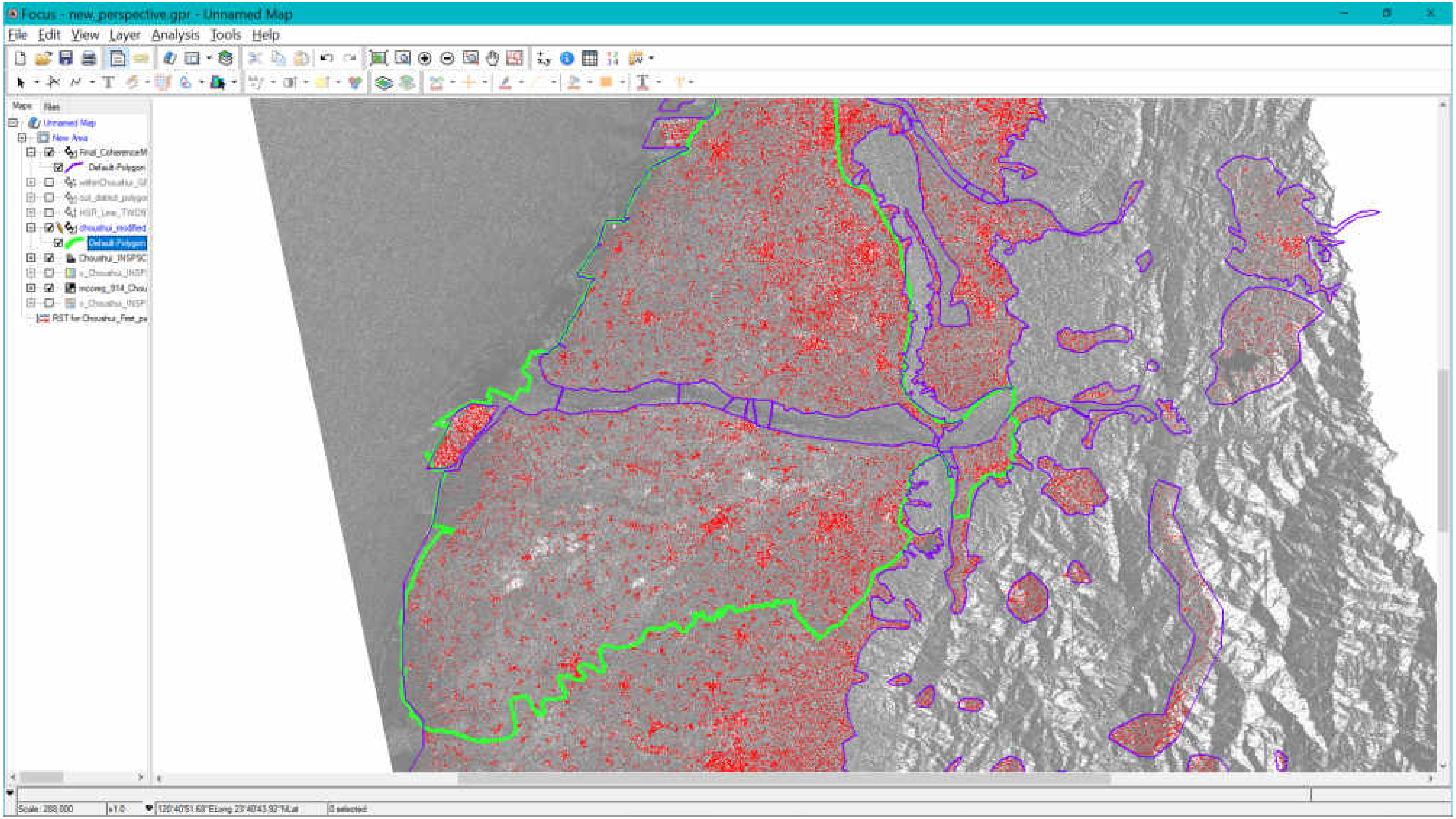
Focus - new_perspective.gpr - Unnamed Map
File Edit View Layer Analysis Tools Help
Unnamed Map
New Area
Final_CoherenceM
Default Polygon
choushui_modified
Default Polygon
Choushui_INSP9C
mcoreg_914_Chou
RST for Choushui_First_pa
Scale: 288,000
120°40'51.68"ELong 23°40'43.92"NLat
0 selected

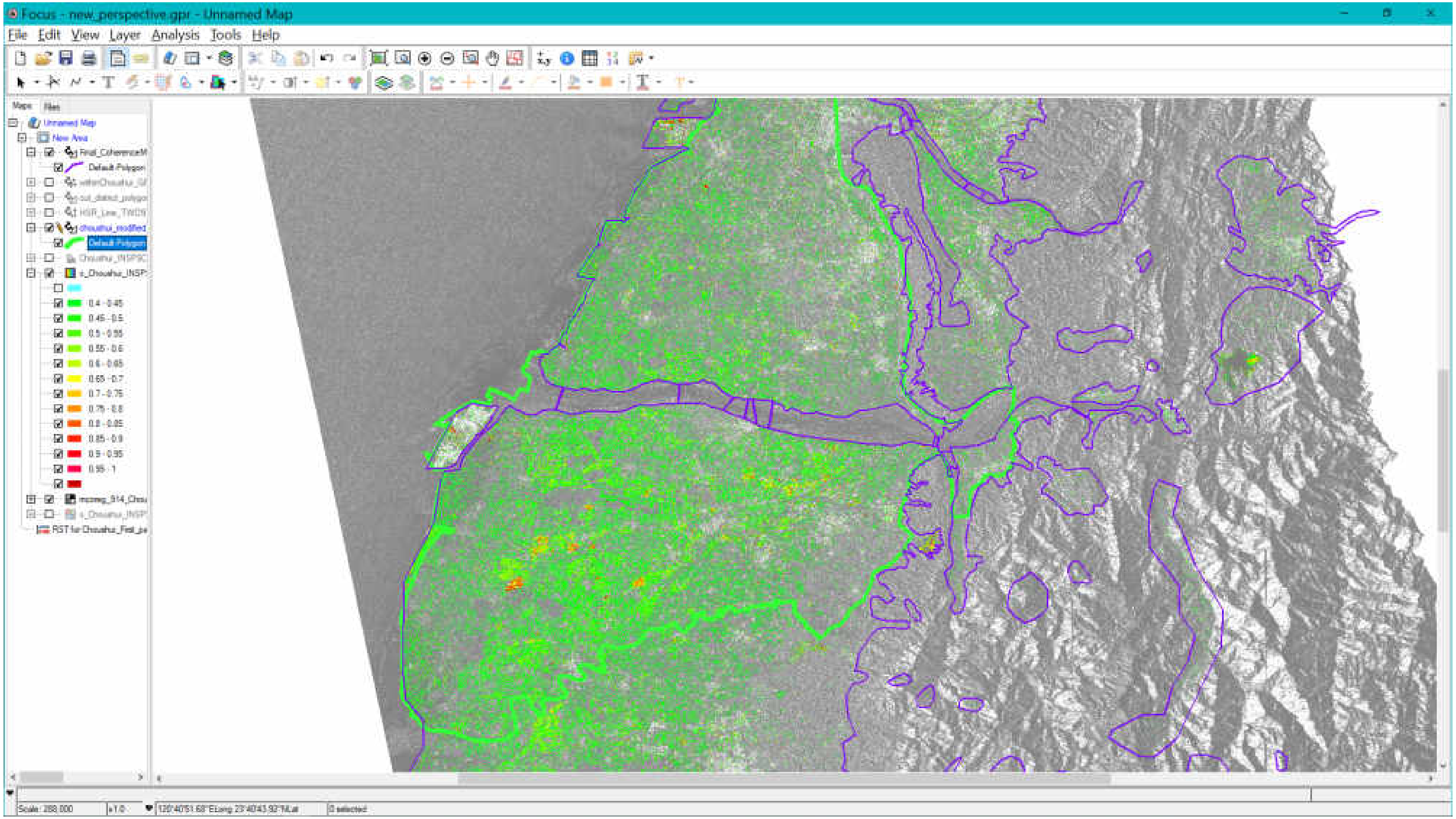
Focus - new_perspective.gpr - Unnamed Map
File Edit View Layer Analysis Tools Help
Maps
Files
Unnamed Map
New Area
Default Polygon
Default Polygon
0.4 - 0.45
0.45 - 0.5
0.5 - 0.55
0.55 - 0.6
0.6 - 0.65
0.65 - 0.7
0.7 - 0.75
0.75 - 0.8
0.8 - 0.85
0.85 - 0.9
0.9 - 0.95
0.95 - 1

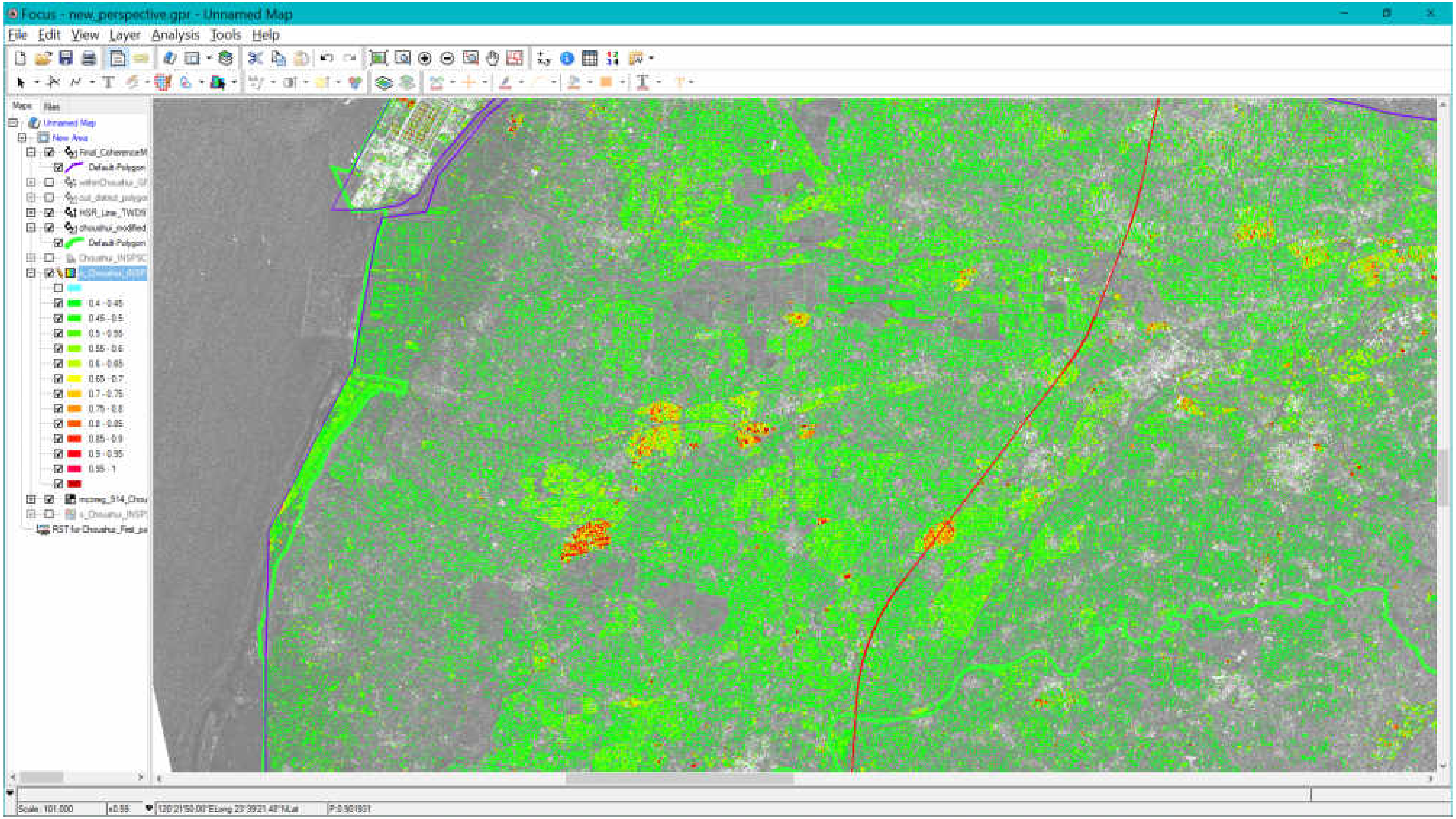
Focus - new_perspective.gpr - Unnamed Map
File Edit View Layer Analysis Tools Help
Unnamed Map
New Area
Default Polygon
Default Polygon
0.4 - 0.45
0.45 - 0.5
0.5 - 0.55
0.55 - 0.6
0.6 - 0.65
0.65 - 0.7
0.7 - 0.75
0.75 - 0.8
0.8 - 0.85
0.85 - 0.9
0.9 - 0.95
0.95 - 1

Phase Unwrapping

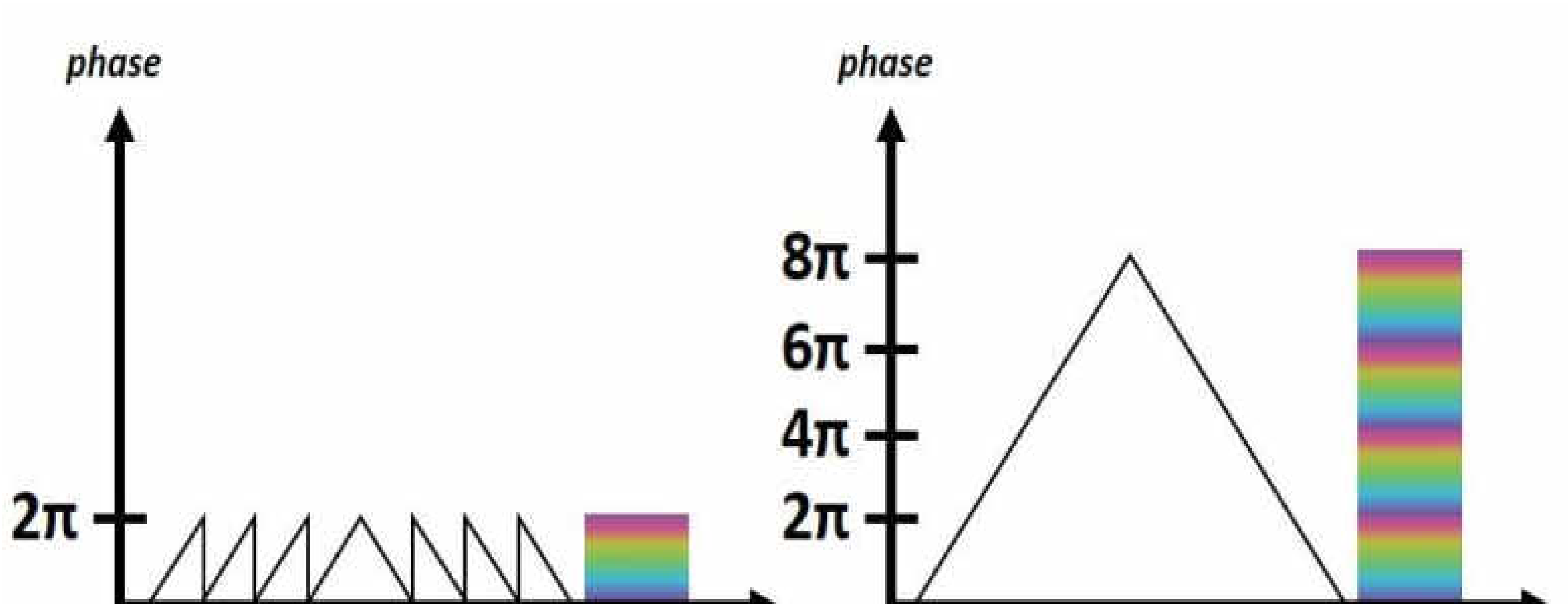

1. Image Pairs Selection
2. Coregistration

Image 1 spatially aligned with **Image 2**, utilizing the ground control points (GCPs)

So that any feature in **Image 1** overlaps as well as possible its footprint in **Image 2**

Image courtesy of Massachusetts Executive Office of Environmental Affairs

Orthophoto image (Master image)

Image courtesy of mPower3/Emerge

Aerial photo image (Slave image)

Image 1 spatially aligned with **Image 2**,

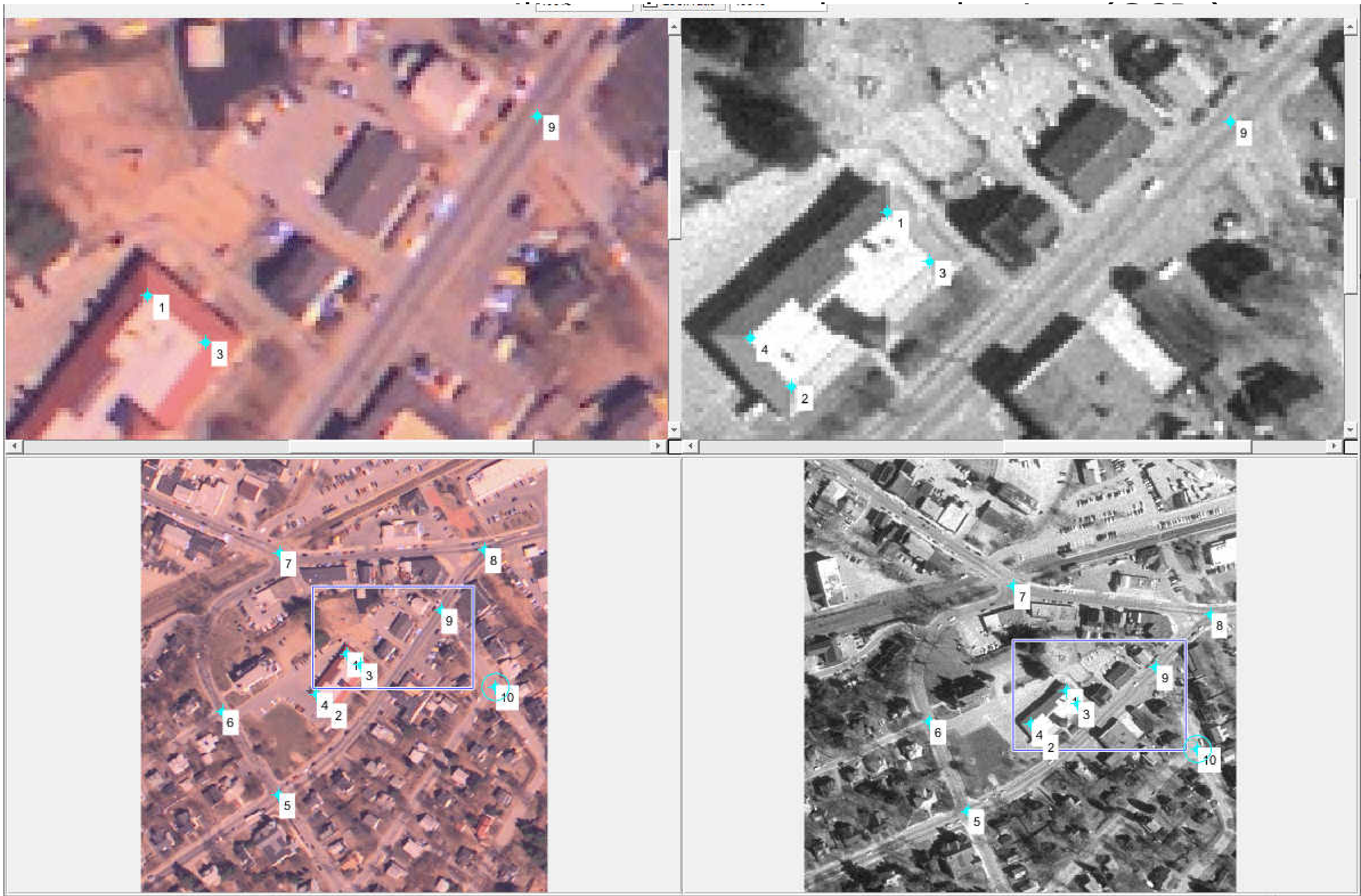

Image 1 spatially aligned with **Image 2**, utilizing the ground control points (GCPs)

So that any feature in **Image 1** overlaps as well as possible its footprint in **Image 2**

Master image

$$C_1(r,a) = A_1(r,a)e^{i\varphi_1(r,a)}$$

Slave image

$$C_2(r,a) = A_2(r,a)e^{i\varphi_2(r,a)}$$

A complex interferogram

$$C_2 C_1^* = A_1 A_2 e^{i(\varphi_2 - \varphi_1)}$$

* is the complex conjugation

Lu, C.-H., Ni, C.-F., Chang, C.-P., Yen, J.-Y., & Chuang, R. Y. (2018). Coherence difference analysis of sentinel-1 SAR interferogram to identify earthquake-induced disasters in urban areas. *Remote Sensing, 10*(8), 1318.

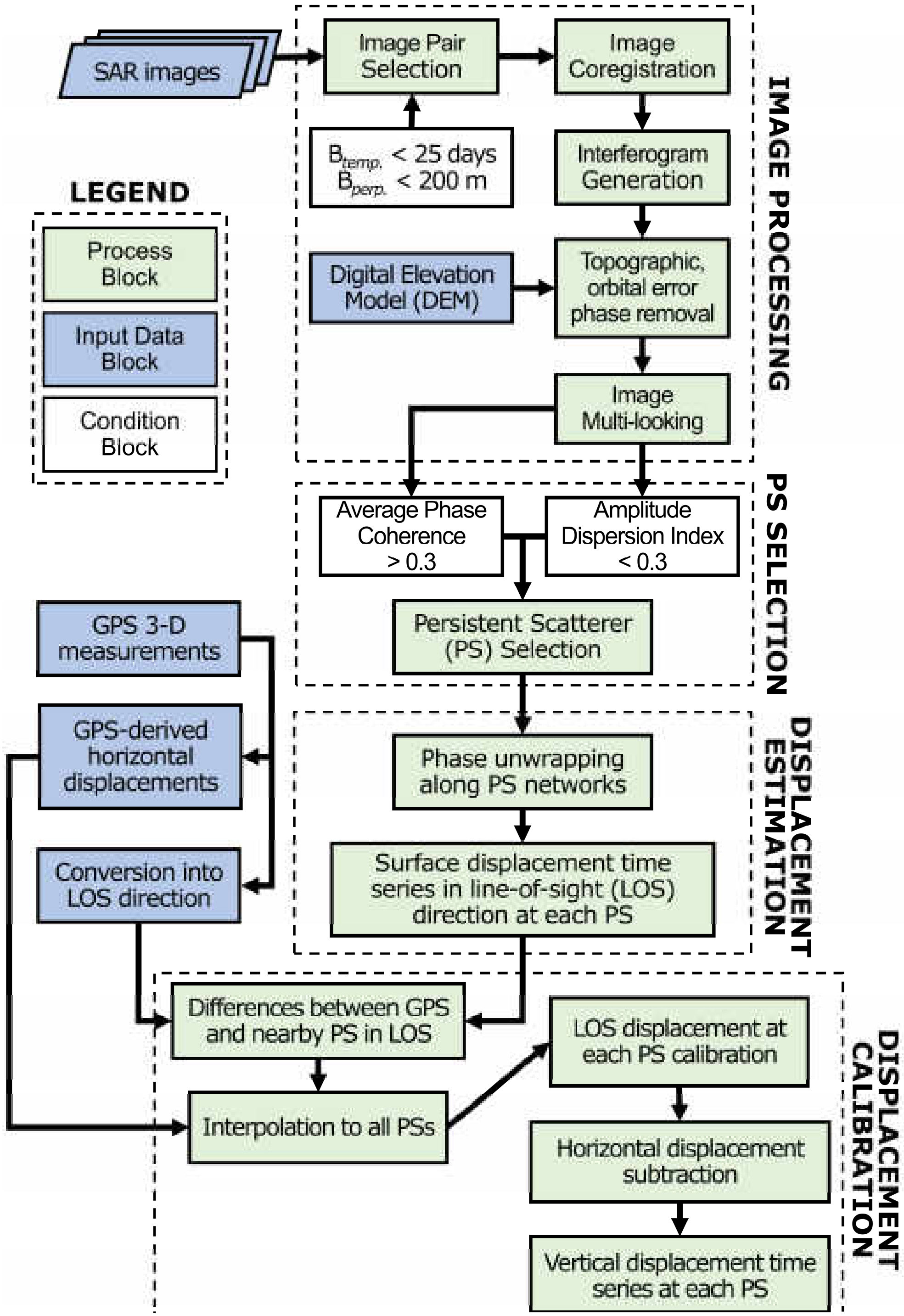
SAR images
Image Pair Selection
Image Coregistration
B_temp. < 25 days
B_perp. < 200 m
Interferogram Generation
Digital Elevation Model (DEM)
Topographic, orbital error phase removal
Image Multi-looking
IMAGE PROCESSING
LEGEND
Process Block
Input Data Block
Condition Block
Average Phase Coherence > 0.3
Amplitude Dispersion Index < 0.3
Persistent Scatterer (PS) Selection
PS SELECTION
GPS 3-D measurements
GPS-derived horizontal displacements
Conversion into LOS direction
Phase unwrapping along PS networks
Surface displacement time series in line-of-sight (LOS) direction at each PS
DISPLACEMENT ESTIMATION
Differences between GPS and nearby PS in LOS
Interpolation to all PSs
LOS displacement at each PS calibration
Horizontal displacement subtraction
Vertical displacement time series at each PS
DISPLACEMENT CALIBRATION